Potential energy curves and transport properties for the interaction of He with other ground-state atoms.

Harry Partridge and James R. Stallcop

NASA Ames Research Center, Moffett Field, CA 94035-1000, USA

Eugene Levin

Eloret Corporation, Moffett Field, CA 94035-1000, USA

Abstract

The interactions of a He atom with a heavier atom are examined for 26 different elements, which are consecutive members selected from three rows (Li – Ne, Na – Ar, and K,Ca, Ga – Kr) and column 12 (Zn,Cd) of the periodic table. Interaction energies are determined using high-quality *ab initio* calculations for the states of the molecule that would be formed from each pair of atoms in their ground states. Potential energies are tabulated for a broad range of interatomic separation distances. The results show, for example, that the energy of an alkali interaction at small separations is nearly the same as that of a rare-gas interaction with the same electron configuration for the closed shells. Furthermore, the repulsive-range parameter for this region is very short compared to its length for the repulsion dominated by the alkali-valence electron at large separations (beyond about 3–4 a_0). The potential energies in the region of the van der Waals minimum agree well with the most accurate results available. The *ab initio* energies are applied to calculate scattering cross sections and obtain the collision integrals that are needed to determine transport properties to second order. The theoretical values of Li–He total scattering cross sections and the rare-gas atom–He transport properties agree well (to within about 1%) with the corresponding measured data. Effective potential energies are constructed from the *ab initio* energies; the results have been shown to reproduce known transport data and can be readily applied to predict unknown transport properties for like-atom interactions.

PACS number(s): 31.15.Dv, 34.20.Cf, 51.20.+d

Typeset using REVTEX

I. INTRODUCTION

The potential energies describing the interaction of atomic and molecular systems are of fundamental importance for understanding of the physical properties of matter.[1] In particular, interaction energies are needed to determine transport properties such as the coefficients of diffusion and viscosity required for studying or modeling the deposition or etching processes for the manufacturing[2] of microelectronic devices. For the most part, the interaction energies that are considered to be reliable have been determined from various experimental information employing semiempirical or empirical representations of the potential energy. However, *ab initio* calculations have progressed sufficiently that for many systems the accuracies of the computed potentials are now useful in analyzing the experimental data.

A primary motivation for this work is to obtain accurate potential energy curves for the determination of transport properties. Our goal is to establish the data base needed to generate effective potential energies for more complex interactions. We have demonstrated[3–5] that the effective potential energies that are constructed from certain interaction energies of He with simple systems can be applied to determine the transport properties for more complex systems with reasonable accuracy.

In this work, we examine the interactions of many different ground-state atoms with a He atom in the ground state. Three consecutive elements of all of the columns of the first row of the periodic chart (i.e., Li–K, Be–Ca, B–Ga, C–Ge, N–As, O–Se, F–Br, and Ne–Kr) are included in this study. The selected interaction partners allow a systematic examination of the effects of increasing atomic size/mass for a given number of valence electrons. Potential energies and certain parameters of their corresponding van der Waals curves are reported for all the above atom–He interactions and, in addition, the Zn–He, and Cd–He interactions.

We do not include the effect of spin-orbit interactions in this study. Although the fine structure splitting is sizable for many of the open-shell systems studied, the effect on the transport properties is small at higher temperatures. The adiabatic potential curves required for applications at low temperatures (e.g., below about 300 K for the transport properties

of the first-row atoms), may be readily determined from the formulation of Hickman *et al.*[6] using the present results and the measured values of the fine-structure constants of the isolated atoms (i.e., by neglecting[7] a small variation with the interatomic separation distance r).

Recent advances in the calculation of interaction energies are discussed and our computational approach is described briefly in the next section. In Sec. III, we present our atom–He potential energies and compare them with the corresponding results of other work. In Sec. IV, our potential energies are applied to calculate scattering cross sections and transport collision integrals; some calculated results are compared with the corresponding measured quantities. A formulation for separating the repulsive and attractive components of the atom–He interaction energies is applied to identify the effective potential energies for interactions of He with open-shell atoms in Sec. V. In Sec. VI, we use the Aufbau method to construct effective potential energies for determining the transport properties of like-atom interactions. A summary of our results and conclusions is contained in Sec. VII.

II. CALCULATION OF INTERACTION ENERGIES

The computational difficulties in determining quantitative representations for weakly interacting systems is well known.[8,9] In particular the basis set requirements are quite severe, requiring diffuse and higher angular momentum functions to describe the dispersion interaction and the compact function to minimize the basis set superposition error (BSSE). A number of authors, however, have demonstrated[10–12] the effectiveness of employing bond functions for describing weakly interacting systems. In particular the results obtained by Tao and co-workers[10,11] are extremely impressive. We have recently examined[13,14] the effectiveness of bond functions for augmenting basis sets. For strongly bound systems, the bond function sets employed did not offer[13] any advantage over augmenting the atom centered basis sets. In fact, they complicated schemes for extrapolating to the complete basis set limit. However, it is worth emphasizing that counterpoise corrected results were consistent even

for very large bond function sets. That is, any limitations in the counterpoise correction are not significant compared with other errors in the calculations.

For weakly bound systems, the improvement has been shown[14] to be spectacular with a cc-pvTZ+bf set giving well depths superior to a doubly-augmented cc-pV5Z basis set. Furthermore, we showed that the bond function results were consistent with the basis set extrapolated results. Again the counterpoise corrected results were reliable at short bond lengths and independent of the size of the bond function set. While we concluded that the +bf results were yielding accurate results for the full potential energy curve, it is clear that the bond functions make little contribution to the interaction energy at the shorter r values, especially using the diffuse functions in the Tao set. We thus prefer using at least a QZ quality basis set, to obtain a reliable description of the repulsive wall.

In the present work, all systems are studied using the coupled cluster singles and doubles approach[15], including a perturbational correction for the triples[16], CCSD(T). For the open-shell systems the RCCSD(T)[17,18] approach is used. For the main group elements only the valence electrons are correlated. For the alkali and alkaline-earth systems, the outer-core electrons of the metal are included in the correlation treatment because of the importance of core-valence contraction of the outer shell.[19] For Zn and Cd, the outer d shell is correlated. For Ga, the $3s, 3p$, and $3d$ electrons are included in the correlation treatment and for Ge the $3d$ electrons are correlated.

Except where noted, the atom-centered, augmented correlation-consistent polarized-valence, aug-cc-pVQZ (aqz), sets of Dunning and co-workers[20–25] are employed. For selected systems, calibration calculations used the augmented quintuple zeta (a5z) sets. For the alkali and alkaline-earths, the primitive sets are partially uncontracted and augmented with compact functions to describe the core-valence correlation. For Ga we employ the QZ set optimized by Bauschlicher.[26] For Ge the QZ set optimized by Ricca[27] is employed with one additional s and p function uncontracted. For Kr the 5Z basis set of Ref. 28 is employed.

The basis sets are augmented with a bond function set at the bond midpoint; the bond function set, designated +bf, is that recommended by Tao and Pan[11]. It consists of three

s and p functions (exponents 0.9, 0.3, and 0.1), two d (0.6 and 0.2) functions, one f (0.3) function, and one g (0.3) function.

All of the results are corrected for BSSE employing the counterpoise method.[29] The calculations are performed using Molpro[30].

III. POTENTIAL ENERGY CURVES

The potential energies

$$V^{\mathrm{He-X}}(r) = E^{\mathrm{He-X}}(r) - E_{\mathrm{BBSE}}(r) - E^{\mathrm{He}} - E^{\mathrm{X}} \qquad (1)$$

for the interaction of He with an atom X have been determined from the calculated energies E for all the systems studied. These results include all the molecular states in the LS coupling scheme that are obtained for the interaction of atoms in their ground states. The results for Σ-state interactions with the atoms of the first three rows of the periodic chart are listed in Tables I – III. The position of the different interactions in these tables is chosen to coincide with the relative position of the heavier element in the periodic table in order to facilitate comparisons w.r.t. the number of valence electrons. In addition, the results for the alkali–He interactions at values of r greater than $15a_0$ are listed in Table IV. The companion results for the Π-state interactions can be obtained from Table V for the first two rows and from Table VI for the third row.

Note that for interactions with P-state atoms, the order of the energies for the molecular states with different symmetry is reversed for helium–hole (electron is needed to fill the valence shell) from that for helium–electron interactions. For example, one notes from Tables I and V that the Π-state energies of B–He lie below the corresponding energies for the Σ state; whereas, for F–He the Σ-state energies are the lowest. These electron-hole pairs can also be identified with certain left-right valence pairs of the periodic table (e.g., carbon and oxygen form a pair for two valence electrons and holes, respectively, in the first row) and hence, from the columns of these pairs in our tabulations for $V(r)$.

The $V(r)$ for Zn–He and Cd–He are contained in Table VII. The tabulated energies illustrate general features that are found for increasing mass/size for atoms with a specific valence number. For example, the $V(r)$ for the interaction with the heavier atom is more repulsive (i.e, $V(r)$ is larger for a given value of r) at small r than the $V(r)$ for the lighter atom. At large r, however, the $V(r)$ for the heavier atom is more attractive (i.e., would lie below the corresponding energy of the lighter atom).

Certain van der Waals parameters that are determined from the curves for the corresponding $V(r)$ of Tables I – VII are listed in Table VIII. This tabulation contains the values of r_0, for which $V(r_0) = 0$, the location r_e of the well minimum, and the depth D_e of the potential energy well.

A. Dispersion Coefficients

The computational approach with bond functions of Sec. II is very effective for determining $V(r)$ at large r; this includes alkali–He interaction energies, which have very large long-range coefficients. We find that the values of $V^{\mathrm{He-Li}}(r)$ in Table IV at large r agree (to within about $0.01\mu E_h$) with the corresponding results obtained using the values of the dispersion coefficients C_{2n} calculated by Spelsberg *et al.*[31] and a long-range expansion of the interaction energy. Furthermore, if the small repulsive exchange contribution is included using the analytical potential function of Eqs. (9) as described in Sec. V, then the good agreement of the values of Tables I and IV with the corresponding results obtained using all values of C_{2n} ($2n$ = 6–12) tabulated in Ref. 31 includes the region of smaller r (i.e, the agreement remains within about 1% for decreasing values of r down to about r_e). A similar good agreement with the corresponding results obtained from the C_{2n} of Ref. 31 is found for Na–He interactions. For K–He interactions, however, the values of r contained in Table IV are not sufficiently large to ascertain the precise long-range contribution; i.e., it is masked by the uncertainty in the repulsive exchange contribution.

The values of $V(r)$ for r larger than those of Tables I – VII are required for the scattering

applications of Sec. IV. The *ab initio* results for energies at large r can be applied to determine sufficiently accurate values of unknown dispersion coefficients C_6^{He-X} for the leading term of a long-range expansion of the interaction energy. The relative values of higher-order coefficients are approximated using the relations

$$\frac{C_8}{C_6} = \frac{3}{2}\left[\frac{< r_a^4 >}{< r_a^2 >} + \frac{< r_b^4 >}{< r_b^2 >}\right] \tag{2a}$$

and

$$\frac{C_{10}}{C_6} = \left[2\frac{< r_a^6 >}{< r_a^2 >} + 2\frac{< r_b^6 >}{< r_b^2 >} + \frac{21}{5}\frac{< r_a^4 >}{< r_a^2 >}\frac{< r_b^4 >}{< r_b^2 >}\right], \tag{2b}$$

which can be derived from the general formulation of Starkshall and Gordon[32] for the interaction of atoms a and b. The quantities $< r^n >$ are the radial expectation values for the atoms and are tabulated by Desclaux.[33]

At large r, the contribution from both the repulsive exchange interaction and the attractive terms of the long-range interaction expansion for the higher-order dispersion coefficients are small; hence, sufficiently accurate values of C_6^{He-X} can be readily extracted from the calculated values of $V(r)$ at large r using only the contribution from the higher-order long-range terms for the C_{2n}^{He-X} obtained from Eqs. (2). For example, the value of C_6^{He-N} determined from the $V^{He-N}(r)$ of Table I is $5.70 a_0^6 E_h$ and agrees fairly well with the value $5.793 a_0^6 E_h$ of Margoliash and Meath.[34].

This approach to determine C_6 and the approximations (2) are also applied in Secs. V and VI below to obtain effective potential energies.

B. Electronic structure of alkali atoms

The effect of the atomic shell structure is very pronounced in the alkali–He (A–He) results of the present calculations. The curves for $V^{He-A}(r)$ are compared with those for the interaction of a rare gas (RG) atom with a He atom in Fig. 1 for r in the repulsive region. Note that the value of the range parameter

$$\rho = \left[\frac{d}{dr}\ln V(r)\right]^{-1} \quad (3)$$

of an exponential repulsive energy for alkali interactions is much smaller at small r compared to its value at large r. At large r, the behavior of $V^{He-A}(r)$ is determined primarily by the interaction of the electrons of the He atom and the diffuse s-valence electron of the alkali atom. At small r, the core electrons of the alkali atom provide the dominant contribution to $V^{He-A}(r)$; consequently, the values of a certain $V^{He-A}(r)$ are close to the values of $V^{He-RG}(r)$ when the RG atom has the same shell structure as the core electrons of the alkali atom. This anomalous behavior of ρ is found only in our results for the A–He interactions. Such abrupt changes in ρ at shell boundaries are expected for the interactions of the other heavier atoms of this work and also the heavier alkali interactions to occur at values of r that are smaller than those of our $V(r)$ tabulation (and consequently, at energies too high to be interest for the present transport calculations).

C. Comparisons of the van der Waals interaction energies

The parameters obtained from the *ab initio* calculations are compared with the results of previous work for the van der Waals region in Tables IX – XII. The $V(r)$ for this region are also compared in Figs. 2 – 4.

Table IX and Fig. 2 show that the results of high-quality accurate *ab initio* calculations agree well with the values of $V^{He-RG}(r)$ of Keil *et al.*[38] that were obtained by combining measured data for scattering, diffusion and other processes with the values of the long-range coefficients. We point out that only the multi-reference configuration interaction (MRCI) and CCSD(T) results from the high-quality calculations of Refs. 36 and 37, respectively, are considered here; the results of earlier less-accurate calculations are discussed in Ref. 37. Note that the a5z values of the present calculation are in agreement with the corresponding values of the a5z results of Ref. 37. The values of $V^{RG-He}(r)$ for Ne–He in Table I and Ar–He in Table II include the r range of Ref. 37 for completeness and to facilitate comparisons with other interactions. Moreover, the present results for these interactions are more suitable for

applications such as those of Sec. IV, since a larger range and some smaller intervals of r are contained in the tabulations.

The values of D_e listed by Ogilvie and Wang[57] for their vibrational analysis are about 2% smaller than the experimental values contained in Table IX. Contrarily, the present values of D_e for Kr–He are slightly larger; this is consistent with arguments[37] that the experimentally derived curves for $V^{He-RG}(r)$ are a little too shallow. We point out that improvements in the calculations will deepen the computed values of $V(r)$; this alone also suggests that the experimental curves are slightly too shallow at larger r (between about 7 and 8 a_0), and correspondingly too repulsive at smaller r.

The error in the computed potentials increases with larger masses. In part, this is due to the slightly larger basis set sensitivity for the heavier systems. The magnitude of the error in the n-particle treatment is unknown, but the Ne–He results suggest that it is small. We suggest that the increase in the difference with the experimentally deduced potentials is largely due to the neglect of scalar relativistic effects. Nevertheless, Table IX and Fig. 2 show that the RG–He theoretical curves from CCSD(T) calculations for the van der Waals region agree with the corresponding experimental results essentially to within the experimental uncertainty even for large interaction partners such as Kr.

Staemmler and Jaquet[47] have used a coupled-electron-pair approximation (CEPA) to obtain O–He interaction energies; the results of their best calculation are listed in Table XI. They have estimated the error in their results from basis set incompleteness; taking their extrapolated values, which account for this error and are listed in Table 2 of Ref. 47, we obtain the values 3.57Å for r_e and $43\mu E_h$ for D_e of the $^3\Sigma^-$ state. These values agree remarkably well with our corresponding values contained in Table VIII.

A CCSD(T) method with bond functions has been used recently by Burcl *et al.*[49] to calculate Cl–He interaction energies. As shown in Table XI and Fig. 3, the present energies are only slightly lower than corresponding results of Ref. 49, which were obtained using a smaller basis set (atz) for Cl. This slight lowering is also found from a comparison of the results of Ref. 48 for Cl–He that have been calculated recently using both atz and aqz

basis sets.The calculations of Ref. 48 were performed, however, without bond functions; the improvement in the value of D_e by adding +bf to the basis set can seen in Table XI.

Lastly, we compare A–He interaction energies of previous calculations with our results. As shown in Fig. 1 and discussed above, the behavior of the A–He repulsive energy at large r is dominated by the valence electron of the alkali atom. Hence, one expects that a one-electron model of the alkali atom that properly accounts for the effects of the core electrons could yield reasonably accurate estimates of the interaction energies at large r. The estimates from the simple models of Patil,[51] Cvetco *et al.*,[52] and Kleinekatöfer *et al.*[54] are included in Table XII. Our results for the A–He systems have shorter bond lengths and larger bond energies compared to their results. This is not surprising, since the core-valence correlation energy is relatively large; e.g., the valence-level binding energy of Na–He is $6.0\mu E_h$ and considerably less than the core-valence result $7.0\mu E_h$ of Table VIII.

Staemmler[55] has used a CEPA method with very large basis sets for the Li atom to determine Li–He interaction energies; he estimates that his results contain nearly all (97%) of the correlation energy. The values shown in Table XII and Fig. 4 are obtained from the extrapolated results that include this small missing correlation and are determined using his calculated correlation energies listed in Table 1 of Ref. 55. The $V^{\mathrm{He-Li}}(r)$ of the present calculation are only slightly lower than these extrapolated results. The predicted values of $V^{\mathrm{He-Li}}(r)$ of Behmenburg *et al.*[56] shown in Fig. 4 and their comparisons[56] with measured spectroscopic data provide further support for the accuracy of our calculations at large r.

The values of $V(r)$ at large r from the present calculation are shown to be among the most accurate currently available; hence, the comparisons of Tables X – XII and Fig. 4 lead to some favorable observations about relatively simple calculations. For example, the calculations[39,46,47,55,58] with CEPA methods yield fairly reliable estimates of $V(r)$ in the van der Waals region. Furthermore, effective core potentials with terms to account for core polarization can provide[42,44,53,56] reasonably accurate results at large r with a relatively small effort.

We conclude the comparisons of this section, by pointing out that certain potential

energy curves that have been deduced from measurements of the total cross section of atomic beams scattered by He gases are not included in the above discussion. The accuracy of the curves obtained from experiments is generally unreliable, however, because cross section data from a limited range of collision energies alone is not sufficient[59] to determine a unique interaction energy. Moreover, the potential data inferred for the van der Waals region may be particularly inaccurate; the structure, which is required for a unique determination of both r_e and D_e, is not found in the He scattering cross sections because the beam energies are too high. The curve for $V^{\mathrm{He-Li}}(r)$, obtained by Dehmer and Wharton[60] from fits to their beam scattering measurements, for the region of the van der Waal well is in qualitative agreement with the present results. For example, they have estimated that the value of r_0 for Li–He lies in the range 6.0 – 6.4Å and, hence, considerably larger than our corresponding result 5.38Å obtained from Table XII. Similarly, the values of r_0 obtained by Aquilanti and coworkers[61–63] from their measurements of the scattering of P-state atoms differ from the corresponding values of Table VIII by amounts up to about 3% for O–He,[61] 8% for F–He,[62] and 7% for Cl–He.[63]

IV. SCATTERING CALCULATIONS

As mentioned above, the cross sections are determined using a quantum mechanical formulation of the elastic scattering in the field of $V(r)$ for each molecular state of the interaction. The phase shifts are calculated at lower collision energy E using the quantum mechanical method presented by Levin *et al.*[64] A semiclassical method[65] is used to determine the phase shifts for E above a threshold energy E_t where the difference in the cross sections between the two methods is less than 3 units in the fourth significant figure.

A. Li–He scattering cross sections

Total cross sections such as those measured in Ref. 60 should provide a test of the repulsive region of our Li–He interaction energy, since the uncertainty in the contribution

to the scattering from the region of large r, where our $V^{He-Li}(r)$ is shown to be accurate in Sec. III, can be considered to be very small. The cross section that is calculated from the $V^{He-Li}(r)$, obtained by combining the discrete values of Tables I and IV with the long-range interaction energy using the extracted values of C_{2n} described in Sec. III, is compared in Fig. 5 with the measured data that has been deconvoluted[60] to remove the effects of target motion. Considering the spread in the experimental data, the calculated cross sections appear to agree well with the measured data at low collision energies, but are about 1% larger at the highest energies. This comparison supports a conclusion that our results for simple systems such as Li–He be applied to calibrate measured cross sections at low energies in order to avoid errors introduced by certain experimental techniques, such as those discussed in Ref. 60.

B. Collision integrals for transport properties

As pointed out in the discussion of Sec. I, the spin-orbit interaction of the electrons must be taken into account for collisions of He with atoms in a P state at low collision energies. The relative contribution from this interaction to transport properties at low T is discussed in Ref. 5. For calculations at higher T, however, the LS coupling approximation used for the calculation of $V(r)$ is adequate. The transport cross sections $\bar{Q}_n(E)$ that would be observed in the laboratory are obtained by averaging over all cross sections $Q_n(E)$ for the molecular states that correspond to dissociation into ground state atoms using the appropriate degeneracy factors. For collisions of He with atoms in a P state,

$$\bar{Q}_n(E) = \frac{1}{3}Q_n^{\Sigma}(E) + \frac{2}{3}Q_n^{\Pi}(E) \tag{4}$$

where Σ and Π are the angular momentum of the molecular states.

For a Maxwell-Boltzmann velocity distribution, the transport properties are obtained[1] from the collision integrals

$$\bar{\Omega}_{n,s}(T) = \frac{F(n,s)}{2(\kappa T)^{s+2}} \int_0^{\infty} e^{-E/\kappa T} E^{s+1} \bar{Q}_n(E) dE. \tag{5}$$

The factor $F(n,s)$ is defined in Ref. 66 and accounts for the normalization to the result for the scattering of unit hard-spheres. The discrete values of $V(r)$ contained in Tables I – VII are combined with the long-range interaction energy obtained from the C_{2n} described in Sec. III to calculate $\Omega_{n,s}(T)$. The values of the transport integrals for diffusion $\tilde{\Omega}_{1,1}(T)$ and viscosity $\tilde{\Omega}_{2,2}(T)$ are listed in Tables XIII – XVI. More extensive results that include the $\tilde{\Omega}_{n,s}(T)$ required to determine other properties such as the thermal diffusion factor or the contribution from higher-order terms are contained in a PAPS document.[67]

C. Comparison of predicted Rare Gas-He transport properties with measured data

We show that the calculated values of $V^{\mathrm{He-RG}}(r)$ in the van der Waals region agree well with the experimental results in Sec. III; hence, a comparison of the transport properties predicted from the calculated values of $V^{\mathrm{He-RG}}(r)$ with the corresponding measured data should provide a test of the accuracy of $V^{\mathrm{He-RG}}(r)$ in the repulsive region.

To calculate the higher-order contributions to the transport properties of a mixture, we apply the matrix formulation of Chapman and Cowling.[68] For example, the binary diffusion coefficient is obtained from[69,70]

$$D(x,T) = \lim_{m\to\infty} D^{(m)}(x,T) \tag{6a}$$

where the quantity x specifies the composition of the mixture and the mth order can be written in the form

$$D^{(m)}(x) = D^{(1)}(T) f^{(m)}(x,T). \tag{6b}$$

The factor $f^{(1)}$ is equal 1 and the the first-order diffusion coefficient can be determined[71] in units of cm^2/s from

$$10^4 p D^{(1)} = 26.287(2\mu)^{-1/2} T^{-3/2} / \Omega_{1,1}^{\mathrm{He-X}}(T); \tag{7}$$

where T is in K, the pressure p is in atmospheres, the reduced mass μ for the collision partners is in amu, and $\Omega_{1,1}$ is in $\mathrm{\AA}^2 = 10^{-16}\ \mathrm{cm}^2$. The values of the physical constants of Cohen and Taylor[72] were used to obtain Eq. (7).

Higher-order values of $D^{(m)}(x,T)$ for $m > 1$ are calculated using the $f^{(m)}(x,T)$ obtained[70] from the A matrix; the matrix elements $a_{i,j}$ are expressed in terms of the collision integrals by Mason[69,70] for m up to fourth-order. Similarly, higher-order values of the binary viscosity coefficient $\eta(x)$ are calculated[70] from the B matrix; the elements $b_{i,j}$ required to obtain second and third-order η from the collision integrals are also available.[73,74]

The determination of the transport properties of a binary mixture requires[1,75] the contributions from the like-atom interactions as well as the contribution from the unlike-atom interactions. A set of like-atom potential energies $V^{b-b}(r)$, which yield transport properties that agree with the best measurements on the corresponding pure gases is selected for our calculations. Accurate *ab initio* energies for He–He yield transport properties with an accuracy that exceeds[76] that of the best measurements. We take the analytical function of Janzen and Aziz,[77] which yields energies that agree well with the results of recent *ab initio* calculations.[78] For the heavier atoms, we select the semiempirical potentials deduced from experimental data by Aziz and Slaman for Ne–Ne,[79] Ar–Ar,[80] and Kr–Kr[80] interactions. The above $V^{b-b}(r)$ yield viscosities that agree[77,79,80] with the accurate measurements of Vogel[81] to within the experimental uncertainty. Furthermore, we find that our values of the pure-gas η calculated from the V^{b-b} agree with the correlation of experimental data obtained by Bich *et al.*[82] to within the uncertainty (0.1–0.3%) of the measurements for T in the range 100–1000K.

The limiting diffusion coefficient

$$D_0(T) = \lim_{x \to 0} D(x,T) \tag{8}$$

where x is the mole fraction of the heavy component provides an accurate test of the calculated values of $V^{\mathrm{He-RG}}$; the factor f obtained from the approximation described above provides a negligible correction to D^1 of Eq. (7) for the interactions studied here. The values D_0^c calculated from the values of $V^{\mathrm{He-RG}}(r)$ listed in Tables I – III are compared with the corresponding D_0^e that are obtained from measured data in Fig. 6. The values of D_0^e from the low-T experiments[38,83] are considered[38] to have an uncertainty of $\pm 0.3\%$. These measured

results have been combined with measured scattering data and other results to determine the interaction potential energies;[38,84] the diffusion calculated from the fitted potential energies is also compared with the present results in Fig. 6. In addition, the high-T prediction[85] obtained from measurements of D and thermal diffusion factor at low-T are also compared in Fig. 6.

Using $V^{\mathrm{He-RG}}(r)$ and $V^{b-b}(r)$, we find that the second-order correction to the first-order viscosity coefficient $\eta^{(1)}(x)$ for equimolar ($x = 0.5$) RG–He mixtures is small (less than 1%). The values of the viscosity η^c calculated from the values of $V^{\mathrm{He-RG}}(r)$ in Tables I – III and $V^{b-b}(r)$ are compared in Fig. 7 with the corresponding results calculated from the potential energies deduced[38] from measured data and the tabulated viscosity data from the correlation of measured data obtained by Kestin *et al.*[86] The predicted η^c for Ne–He interactions agrees with the η^e of Ref. 86 to within the stated[86] accuracy ±0.5% of the fit for T below about 700 K; whereas, the agreement for Ar–He and Kr–He lies within the fit accuracy ±0.4% for T above 300–400 K.

One can conclude from the above comparisons with measured data that the calculated values of $V^{\mathrm{He-RG}}(r)$ would yield transport properties that are accurate to within about 1%. In addition, one might conclude that the $V^{\mathrm{He-RG}}(r)$ may be slightly too repulsive at small r and that this error increases with increasing mass of the atom. This latter conclusion is consistent with our arguments presented in Sec. III.

V. EFFECTIVE POTENTIAL ENERGIES

The accurate determination of atom–atom transport properties requires a large computational effort, especially when a multitude of molecular states are involved in the collisions. On the other hand, the high-temperature transport properties are dominated by the high-spin states with repulsive interactions. Mason and coworkers[87,88] have devised effective potential energies $V_e(r)$ that reproduce measured transport properties for repulsive interactions and are specified by parameters that satisfy certain combining relations. One expects

that the correlation of Ref. 88 can be extended to include many atom–atom interactions. We have shown[4] that an analogous approach based on theoretical results yields reasonably accurate transport data for known atom-atom interactions. This approach allows the transport properties of complex interactions to be readily predicted from the $V(r)$ for the atom–He interactions described above.

In the following work, we adopt a functional form for the atom–He interaction energy to separate the *ab initio* energies into repulsive and attractive components and then use the components to determine a unique $V_e(r)$ for the interaction of He with atoms in a P state. The formulation and results of this section are required for the applications of the following section.

We find that the potential function developed by Tang and Toennies[89] provides a good description of the Van der Waals interactions such as those for the atom–He described above. The interaction energy is expressed as a sum

$$V(r) = V_{SR}(r) + V_{DLR}(r) \tag{9a}$$

of a short-range repulsive (predominantly Pauli exchange) energy

$$\ln(V_{SR}) = a - r/\rho \tag{9b}$$

and a damped long-range attractive energy

$$V_{DLR}(r) = -\sum f_{2n}(r/\rho)\frac{C_{2n}}{r^{2n}} \tag{9c}$$

where f_{2n} is obtained from an incomplete gamma function[90] of order $2n+1$; i.e.,

$$f_{2n}(x) = 1 - \exp(-x)\sum_{k=0}^{2n}\frac{x^k}{k!}. \tag{9d}$$

Higher-order ($2n > 10$) dispersion coefficients are obtained from recursion relations

$$C_{2n+2} = (C_{2n}/C_{2n-2})^3 C_{2n-4}. \tag{10}$$

As described in Sec. III, the leading dispersion coefficient C_6 can be readily determined from the calculated $V(r)$ at a value of r that is sufficiently large such that the contribution

to the interaction from higher-order terms is small. The values of C_6 are determined in this manner assuming that the higher-order contribution to $V(r)$ is obtained from the C_8 and C_{10} terms using Eqs. (2) and, in addition, by selecting a value r large enough to assure that this contribution does not exceed 25%.

The short-range parameters a and ρ of Eq. (9b) are then determined from a least-squares fit to $\ln V_{SR}(r)$ by an iterative procedure.[3] The values of V_{SR} for this fit are obtained from the difference $V(r) - V_{DLR}(r)$ using the calculated values of Tables I – VII, the value of C_6 described in Sec. III and the long-range result of combining Eqs. (9c), and (9d). All the higher-order terms for $2n = 8$–16 are included in the expansion (9c); the values of the higher-order C_{2n} are calculated using Eqs. (2) and (10). From this description, one notes that the fitted analytical potential function (9) is specified by three parameters a, ρ and C_6. These parameters for the interactions He with S-state atoms are listed in Table XVII.

The results of the fit for $\ln V_{SR}(r)$ are illustrated in Fig. 8 for the RG–He interactions and the interaction of He with the nitrogen series (atoms of column 15 of the periodic table). Note that an exponential (9b) provides a fairly good fit because the values of $\ln V_{SR}(r)$ that are determined from the calculated values of $V(r)$ in the manner described above are nearly linear in r. From this linearity, we point out that the functional form (9) can be used to determine fairly accurate curves for $V(r)$ from a small number of data points. Note further that the value of ρ is a little shorter for the RG atoms compared to the nitrogen series and that the values of ρ for the last two members of the valence column are nearly the same. From Table XVII the difference in ρ for the P-As and Ar-Kr pairs is found to be only about $0.02a_0$ and $0.03a_0$, respectively.

For collisions of He with atoms in a P state, we construct a $V_e(r)$ that reproduces the $\tilde{Q}_n(E)$ of Eq. (4) for the applications of Sec. VI. At high E, the dominant contribution to Ω comes from the region of small r where V can be represented well by an exponential form. From the analysis and computed results of Monchick[91] for the collision integrals for an exponential potential, one finds that the collision integrals can be expressed in the form

$$\Omega_{n,s}(T) = (\alpha\rho)^2 C_{n,s}(\alpha) \tag{11a}$$

where

$$\alpha = a + \tau \tag{11b}$$

and $\tau = -\ln(kT)$. The quantity $C_{n,s}(\alpha)$ varies slowly with α and is tabulated in Ref. 91. Hence, it follows from Eqs. (4) and (11), that the repulsive parameters of V_e satisfy

$$(a + \tau)\rho \approx \left[\frac{1}{3}[(a^{\Sigma} + \tau)\rho^{\Sigma}]^2 + \frac{2}{3}[(a^{\Pi} + \tau)\rho^{\Pi}]^2\right]^{\frac{1}{2}}. \tag{12}$$

The values of the repulsive parameters appearing on the r.h.s of Eq. (12) are determined from the values of $V(r)$ for the Σ and Π states, using the procedure outlined above and ignoring the small contribution from the quadrupole moment of the P-state atom.

The value of ρ^{Σ} is found to be close to the value of ρ^{Π} for the P-state interactions of Tables I – VI. From the result of expanding Eq. (12) in temperature, we find that the degeneracy weighted mean of $\ln V_{SR}$ yields a satisfactory approximation to determine V_e at high temperatures where the scattering is dominated by the region of r for which the interaction potentials are repulsive. At low temperatures, one must also include the contribution to Ω from V_{DLR} in constructing V_e. At temperatures of present interest (above 300K), this contribution is small and can be accounted for by taking the weighted mean of the long-range interactions (or equivalently, by taking the weighted mean of the long-range coefficients to represent the interactions at large r).

VI. AUFBAU POTENTIAL ENERGIES FOR LIKE-ATOM INTERACTIONS

Combining relations have been devised[92] that relate the van der Waals parameters of RG interactions. A method has been developed[93] that uses the combining relations of Smith[94] to determine accurate values of atom–atom interaction energies from the $V(r)$ of simpler systems when the values of the long-range coefficients are known. Recently, we have extended[3] this method to include molecular interactions; in particular, we have developed

procedures that allow the determination of V_e for molecular systems from the data for simpler systems with He interaction partners. In this section, we apply the general formulations for the Aufbau method of Ref. 3 to determine the $V_e^{X-X}(r)$ for the interactions of like atoms from the $V_e^{He-X}(r)$ of Sec. V.

As described in Ref. 3, $V_e^{b-b}(r)$ for determining transport data for $b-b$ interactions can be readily constructed (built-up) using the following Aufbau procedure. First, two pairs of repulsive parameters a and ρ are determined[93] using the form (9) from the known quantities $V^{a-a}(r)$ and $V^{b-a}(r)$, where the superscript a represents a relatively simple system such as He, and known long-range coefficients. Then, the repulsive parameters that describe $V_{SR}^{b-b}(r)$ are calculated from the combining relations

$$\rho^{b-b} = 2\rho^{b-a} - \rho^{a-a} \tag{13a}$$

and

$$(a^{b-b} - \ln\rho^{b-b})\rho^{b-b} = 2(a^{b-a} - \ln\rho^{b-a})\rho^{b-a} - (a^{a-a} - \ln\rho^{a-a})\rho^{a-a}. \tag{13b}$$

Finally, $V_e^{b-b}(r)$ is obtained using Eqs. (9) to combine $V_{SR}^{b-b}(r)$ and the $V_{DLR}^{b-b}(r)$ that is calculated from the long-range coefficients.

As in the atom–molecule method of Ref. 3, the system a represents He for the applications here; the input data required for $V^{He-He}(r)$ is determined from the potential function of Janzen and Aziz,[77] which is based on the results of calculations[95] with symmetry-adapted perturbation theory (SAPT) and agrees well with the results of a recent supermolecule calculation.[78] Similarly, the system b represents the the heavier atom denoted by X above; the input data required for $V^{He-X}(r)$ is determined from the calculated data of Tables I – VII and the long-range interaction energy as described in Sec. V. The parameters of $V_{SR}^{X-X}(r)$ is then determined from the parameters of the input data using Eqs. (13); the final step to obtain $V_e^{X-X}(r)$ using Eqs. (9) requires the values of C_{2n}^{X-X}.

Since the value of C_6^{He-X} can be determined from the calculated $V^{He-X}(x)$ as described in Sec. III, the value of C_6^{X-X} can be readily obtained from the well-known combination rule[96]

$$\frac{\alpha^{He}\alpha^{X}}{C_6^{He-X}} = \frac{1}{2}\left[\frac{\alpha^{He}\alpha^{He}}{C_6^{He-He}} + \frac{\alpha^{X}\alpha^{X}}{C_6^{X-X}}\right] \tag{14}$$

which has been found[97] to be accurate to about 0.5%. The quantity α is the polarizability of the atom; its values are obtained from calculations.[98-100] The value of C_6^{He-He} is also taken from the accurate calculations of Ref. 98. The higher-order C_{2n}^{X-X} can then be obtained using the approximations described in Secs. III and V.

The accuracy of the C_6 obtained in the above manner is considered to be sufficient for the applications of this section. For example, the value of C_6^{N-N}, obtained using Eq. (14) and the procedure described in Sec. III, is $24.0a_0^6E_h$ and agrees well with the value[101] $24.12a_0^6E_h$ determined from oscillator strength, photoabsorption, and high-energy inelastic scattering data.

The parameters for V_e that are obtained from the Aufbau method and the C_{2n} describe above are listed in Table XVIII for atoms in S states.

We have also developed[3] a simpler method that is based on a universal potential energy function that is derived from an accurate He–He interaction energy.[77] The calculated values of V^{He-N} are shown to be described well by this universal function in Figs. 11 and 12 of Ref. 3. Using this method, the transport properties can be readily obtained from the Lennard-Jones parameters σ and ϵ (which are the same as the quantities r_0 and D_e, respectively) and the expansion coefficients of a universal collision integral contained in Table IV of Ref. 3. These Lennard-Jones parameters have been determined from the V_e for systems studied here and are listed in Table XIX. This latter approach has been tested[4] for like–atom interactions where the transport properties are known accurately from detailed theoretical calculations. We have shown[4] that the diffusion and viscosity collision integrals for B–B, C–C, and O–O can be obtained quite accurately from the corresponding values for N–N interactions using Aufbau potential energy data.

VII. SUMMARY AND CONCLUSIONS

Accurate values of the $V(r)$ for the complex formed from the atoms of He and heavier elements are calculated using a CCSD(T) method with a basis set that includes bond functions. The selection of elements allows a study of the effects of increasing size for atoms with open and closed valence shells containing s or p electrons. For example, the results are applied to show that the value of the repulsion parameter for $V^{\mathrm{He-A}}(r)$ at small r is primarily determined by the interaction of the electrons of He with those of the alkali core. The van der Waals interaction energy for Li–He is very shallow and agrees well with the results of the best calculations in the literature. The calculated results for the total Li–He scattering cross section agrees to within 1% with corresponding results measured at high collision energies with atomic beams.

We show that the values of $V^{\mathrm{He-RG}}(r)$ calculated for the van der Waals region agree well (roughly to within the experimental uncertainty) with the corresponding potential energy curves that were obtained from fits to accurate data from the measurements of several different processes. Furthermore, our calculated transport coefficients for diffusion and viscosity agree to within about 1% with the correlations obtained from numerous measurements.

Our calculated energies are used to judge the accuracy of simple computational models. For example, we find that one-electron models can yield reasonably accurate energies for alkali interactions in the van der Waals region. Likewise, we find that calculations, with effective core potentials to represent the short-range Pauli repulsion and long-range core polarization terms, can be used to readily obtain the interaction energy at large r.

We have applied our potential energies to calculate collision integrals accurately using methods based on a quantum mechanical description of the scattering. All values required to determine the transport properties of a gas mixture to second order are tabulated. From the comparisons of theoretical and experimental scattering results in Sec. IV, we conclude that tabulated collision integrals will yield transport properties for the He-atom systems that are accurate to within about 1%, even for the heavier systems where relativistic effects

are neglected. Furthermore, the low-energy scattering results that are determined from the calculated values of $V(r)$ for interactions of He with atoms in the S state and small mass should provide accurate calibrations for future scattering measurements.

The calculated results provide the atom–He interaction energies required for the construction of V_e for predicting unknown transport properties. We have tabulated the parameters required to determine like-atom transport properties from universal formulations. Recent studies indicate that fairly accurate transport properties for interactions involving large molecules can be obtained from effective potential energies that are constructed from the atom–He results of Sec. V using additive methods. Furthermore, we point out that the Aufbau method of Sec. VI can be used to readily obtain V_e for the interaction of the large molecules.

ACKNOWLEDGMENTS

Support to Eugene Levin was provided by Contract NAS2-99092 from NASA to the Eloret Corporation.

REFERENCES

[1] J. O. Hirschfelder, C. F. Curtiss, and R. B. Bird, *Molecular Theory of Gases and Liquids* (Wiley-Interscience, New York, 1964).

[2] *Computational Modeling in Semiconductor Processing*, edited by M. Meyyapan (Artech House, Boston, 1995).

[3] J. R. Stallcop, H. Partridge, and E. Levin, Phys. Rev. A **62**, 062709 (2000).

[4] J. R. Stallcop, H. Partridge, A. Pradhan, and E. Levin, J. Thermophys. Heat Transfer **14**, 480 (2000).

[5] E. Levin, J. R. Stallcop, and H. Partridge, Theor. Chem. Acc. **103**, 518 (2000).

[6] A. P. Hickman, M. Medikeri-Naphade, C. D. Chapin, and D. L. Heustis, Phys. Rev. A **61**, 4633 (1997).

[7] J. S. Cohen and B. Schneider, J. Chem. Phys. **61**, 3230 (1974).

[8] B. Liu and A. D. McLean, J. Chem. Phys. **91**, 2348 (1989).

[9] T. Helgaker, W. Klopper, H. Koch, and J. Noga, J. Chem. Phys. **106**, 9639 (1997).

[10] F.-M. Tao, J. Chem. Phys. **100**, 3645 (1994).

[11] F.-M. Tao and Y.-K. Pan, J. Chem. Phys. **97**, 4989 (1992).

[12] H. Koch, B. Fernandez, and O. Christiansen, J. Chem. Phys. **108**, 2784 (1998).

[13] C. W. Bauschlicher and H. Partridge, J. Chem. Phys. **109**, 4707 (1998).

[14] H. Partridge and C. W. Bauschlicher, Mol. Phys. **96**, 705 (1999).

[15] R. J. Bartlett, Annu. Rev. Phys. Chem. **32**, 359 (1981).

[16] K. Raghavachari, G. W. Trucks, J. A. Pople, and M. Head-Gordon, Chem. Phys. Lett. **157**, 479 (1989).

[17] P. J. Knowles, C. Hampel, and H.-J. Werner, J. Chem. Phys. **99**, 5219 (1993).

[18] J. D. Watts, J. Gauss, and R. J. Bartlett, J. Chem. Phys. **98**, 8718 (1993).

[19] H. Partridge, "Core Valence Energy" in *Encyclopedia of Computational Chemistry*, edited by H. F. Schaefer (J. Wiley and Sons Ltd., London, 1998).

[20] T. H. Dunning, J. Chem. Phys. **90**, 1007 (1989).

[21] R. A. Kendall, T. H. Dunning, and R. J. Harrison, J. Chem. Phys. **96**, 6796 (1992).

[22] D. E. Woon and T. H. Dunning, J. Chem. Phys. **98**, 1358 (1993).

[23] D. E. Woon, J. Chem. Phys. **100**, 2838 (1994).

[24] A. K. Wilson, D. E. Woon, K. A. Peterson, and T. H. Dunning, J. Chem. Phys. **110**, 7667 (1999).

[25] D. E. Woon, K. A. Peterson, and T. H. Dunning, unpublished.

[26] C. W. Bauschlicher, J. Phys. Chem. A **102**, 10424 (1998).

[27] A. Ricca and C. W. Bauschlicher, J. Phys. Chem. A **103**, 449 (1999).

[28] C. Heineman, W. Koch, and H. Partridge, Chem. Phys. Lett. **286**, 31 (1998).

[29] S. F. Boys and F. Bernardi, Mol. Phys. **19**, 533 (1970).

[30] MOLPRO 96 is a package of *ab initio* programs written by H.-J. Werner and P. J. Knowles, with contributions from J. Almlöf, R. D. Amos, M. J. O. Deegan, S. T. Elbert, C. Hampel, W. Meyer, K. Peterson, R. Pitzer, A. J. Stone, and P. R. Taylor. The closed shell CCSD program is described in C. Hampel, K. Peterson, and H.-J. Werner, Chem. Phys. Lett. **190**, 1 (1992).

[31] D. Spelsberg, T. Lorenz, and W. Meyer, J. Chem. Phys. **99**, 7845 (1993).

[32] G. Starkshall, and R. G. Gordon, J. Chem. Phys. **56**, 2801 (1972).

[33] J. P. Desclaux, Atomic Data and Nuclear Data Tables 12, 311 (1973).

[34] D. J. Margoliash and W. J. Meath, J. Chem. Phys. 68, 1426 (1978). 64, 3063 (1976).

[35] J. Komasa, J. Chem. Phys. 110, 7909 (1999).

[36] J. van de Bovenkamp, T van Mourik, and F. B. Duijneveld, Mol. Phys. 97, 487 (1999).

[37] S. M. Cybulski and R. R. Toczyłowski, J. Chem. Phys. 111, 10520 (1999).

[38] M. Keil, L. J. Danielson, and P. J. Dunlop, J. Chem. Phys. 94, 296 (1991).

[39] R. A. Chiles and E. Dykstra, Chem. Phys. Lett. 85, 447 (1982).

[40] I. C. Hayes, G. J. B. Hurst, and A. J. Stone, Mol. Phys. 53, 107 (1984).

[41] A. W. K. Leung and W. H. Beckenridge, J. Chem. Phys. 111, 9197 (1999).

[42] E. Czuchaj, H. Stoll, and H. Preuss, J. Phys. B 20, 1487 (1987).

[43] D. J. Funk, W. H. Beckenridge, J. Simons, and G. Chałasiński, J. Chem. Phys. 91, 1114 (1989).

[44] E. Czchaj, R. Rebentrost, H. Stoll, and H. Preuss, Chem. Phys. 138, 303 (1989).

[45] H. Lavendy, J. M. Robbe, and E. Roueff, Astron. Astrophys. 241, 317 (1991).

[46] V. Staemmler and D. R. Flower, J. Phys. B 24, 2343 (1991).

[47] V. Staemmler and R. Jaquet, Chem. Phys. 92, 141 (1985).

[48] F.Y. Naumkin and F. R. W. McCourt, J. Chem. Phys. 108, 9301 (1998).

[49] R. Burcl, R. V. Krems, A. A. Buchachenko, M. M. Szczęśniak, G. Chałasiński, and S. M. Cybulski, J. Chem. Phys. 109, 2144 (1998).

[50] G. Das and A. C. Wahl, Phys. Rev. A 4, 825 (1971).

[51] S. H. Patil, J. Chem. Phys. 94, 8089 (1991).

[52] D. Cvetko, A. Lausi, A. Morgante, F. Tommasini, P. Cortona, and M. G. Dondi, J. Chem. Phys. 100, 2052 (1994).

[53] E. Czcuhaj, F. Rebentrost, H. Stoll, and H. Preuss, Chem. Phys. 196, 37 (1995).

[54] U. Kleinekatöfer, K. T. Tang, J. P. Toennies, and C. L. Yang, Chem. Phys. Lett. 249, 257 (1996).

[55] V. Staemmler, Z. Phys. D 39, 121 (1997).

[56] W. Behmenburg, A. Makonnen, A. Kaiser, F. Rebentrost, V. Staemmler, M. Jungen, G. Peach, A. Devdariani, S. Tserkonyi, A. Zagrebin, and E. Czuchaj, J. Phys. B 29, 3891 (1996).

[57] J. F. Ogilvie and F. Y. H. Wang, J. Mol. Struct. 291, 313 (1993).

[58] M. Jungen, and V. Staemmler, J. Phys. B 21, 463 (1988).

[59] J. P. Toennies, Faraday Discussions Chem. Soc. 55, 129 (1973).

[60] P. Dehmer and L. Wharton, J. Chem. Phys. 57, 4821 (1972).

[61] V. Aquilanti, R. Candori, and F. Pirani, J. Chem. Phys. 89, 6157 (1988).

[62] V. Aquilanti, R. Candori, D. Cappelleti, E. Luzzatti, and F. Pirani, Chem. Phys. 145, 293 (1990).

[63] V. Aquilanti, D. Cappelletti, V. Lorent, E. Luzzatti, and F. Pirani, J. Phys. Chem. 97, 2063 (1993).

[64] E. Levin, D. W. Schwenke, J. R. Stallcop, and H. Partridge, Chem. Phys. Lett. 227, 669 (1994).

[65] J. R. Stallcop, H. Partridge, and E. Levin, J. Chem. Phys. 95, 6429 (1991).

[66] E. Levin, H. Partridge, and J. R. Stallcop, J. Thermophys. Heat Transfer 4, 469 (1990).

[67] See AIP document No. xxx for the tabulation of 9 different $\Omega_{n,s}(T)$ for the various interactions studied. The additional values of this document, for example, allow the determination of $D(T)$ to third order and $\eta(T)$ to second order.

[68] S. Chapman and T. G. Cowling, *The Mathematical Theory of Non-Uniform gases*, 3rd ed. (Cambridge University Press, New York, 1970).

[69] E. A. Mason, J. Chem. Phys. **22**, 169 (1954).

[70] E. A. Mason, J. Chem. Phys. **27**, 75 (1957).

[71] H. Partridge, J. R. Stallcop, and E. Levin, "Potential Energies and Collision Integrals for the Interactions of Air Components. I. *Ab initio* Calculation of Potential Energies and Neutral Interactions," *Molecular Physics and Hypersonic Flows*, edited by M. Capitelli (Kluwer Academic Publishers, Dordrecht, 1996), pp. 323–338.

[72] E. R. Cohen and B. N. Taylor, J. Phys. Chem. Ref. Data **17**, 1795 (1988).

[73] S. C. Saxena and R. K. Joshi, Physica (Amsterdam) **29**, 871 (1965).

[74] R. K. Joshi, Phys. Lett. **15**, 32 (1965).

[75] G. C. Maitland, M. Rigby, E. B. Smith, and W. A. Wakeham, *Intermolecular Forces. Their Origin and Determination* (Oxford University Press, Oxford, 1981).

[76] R. A. Aziz, A. R. Janzen, and M. R. Moldover, Phys. Rev. Lett. **74**, 1586 (1995).

[77] A. R. Janzen and R. A. Aziz, J. Chem. Phys. **107**, 914 (1997).

[78] T. van Mourik and T. H. Dunning, J. Chem. Phys. **111**, 9248 (1999).

[79] R. A. Aziz and M. J. Slaman, Chem. Phys. **130**, 187 (1989).

[80] R. A. Aziz and M. J. Slaman, Mol. Phys. **58**, 679 (1986).

[81] E. Vogel, Ber. Bunsenges. Phys. Chem. **88**, 997 (1984).

[82] E. Bich, J. Millat, and E. Vogel, J. Phys. Chem. Ref. Data **19**, 1289 (1989).

[83] P. S. Arora, H. L. Robjohns, and P. J. Dunlop, Physica (Amsterdam) **95A**, 561 (1979).

[84] R. A. Aziz, P. W. Riley, U. Buck, G. Maneke, J. Schleusener, G. Scoles, and U. Valbusa, J. Chem. Phys. **71**, 2637 (1979).

[85] P. J. Dunlop and C. M. Bignell, Int. J. Thermophys. **18**, 939 (1997).

[86] J. Kestin, K. Knierim, E. A. Mason, B. Najafi, S. T. Ro, and M. Waldman, J. Phys. Chem. Ref. Data **13**, 229 (1984).

[87] J. Bzowski, E. A. Mason, and J. Kestin, Int. J. Thermophys. **9**, 131 (1988).

[88] J. Bzowski, J. Kestin, E. A. Mason, and F. J. Uribe, J. Phys. Chem. Ref. Data **19**, 1179 (1990).

[89] K. T. Tang and J. P. Toennies, J. Chem. Phys. **80**, 3726 (1984).

[90] A. Erdélyi, W. Magnus, F. Oberhettinger, and F. G. Tricomi, *Higher Transcendental Functions* (McGraw Hill, New York, 1953), Vol. II, Chap. 9.

[91] L. Monchick, Phys. Fluids **2**, 695 (1959).

[92] K. T. Tang and J. P. Toennies, Z. Phys. D : At., Mol. Clusters **1**, 91 (1986).

[93] J. R. Stallcop, C. W. Bauschlicher, H. Partridge, S. R. Langhoff, and E. Levin, J. Chem. Phys. **97**, 5578 (1992).

[94] F. T. Smith, Phys. Rev. A **5**, 1708 (1972).

[95] T. Korona, H. L. Williams, R. Bukowski, R. Jeziorski, and K. Szalewicz, J. Chem. Phys. **106**, 5109 (1997).

[96] H. L. Kramer and D. R. Herschbach, J. Chem. Phys. **53**, 2792 (1970).

[97] A. J. Thakkar, J. Chem. Phys. **81**, 1919 (1984).

[99] D. M. Bishop and J. Pipin, Int. J. Quantum Chem. **45**, 349 (1993).

[99] H. Werner and W. Meyer, Phys. Rev. A **13**, 13 (1976).

[100] E. Reinsch and W. Meyer, Phys. Rev. A **14**, 915 (1976).

[101] G. D. Zeiss and W. J. Meath, Mol. Phys. **33**, 1155 (1977).

TABLES

TABLE I. Potential energies (in μE_h) for Σ states.

$r(a_0)$	$LiHe(^2\Sigma^+)$	$BeHe(^1\Sigma^+)$	$BHe(^2\Sigma^+)$	$CHe(^3\Sigma^-)$	$NHe(^4\Sigma^-)$	$OHe(^3\Sigma^-)$	$FHe(^2\Sigma^+)$	$NeHe(^1\Sigma^+)$
1.75	174316.06							
2.00	94854.24							
2.25	53753.20							
2.50	32625.73	73225.98	231648.11	41825.30	116058.20	163234.55	52974.71	96903.89
2.75	21763.18	57787.94	136966.06	28357.35	73445.72	99755.84	30251.96	54239.02
3.00	16065.39	45695.72	98034.00	18648.05	45774.42	60571.98	16926.55	30059.86
3.25	12885.19	35653.68	69186.91	11835.13	28116.36	36566.32	9223.78	16460.98
3.50	10881.19	27297.27	48349.82	7227.80	17021.98	21936.80	4854.82	8875.81
3.75	9402.18	20496.00	33531.46	4225.95	10148.21	13062.78	2431.99	4686.49
4.00	8155.34	15117.98	23107.56	2339.47	5945.09	7706.18	1124.29	2400.76
4.25	7026.71	10970.32			3408.57			
4.50	5984.78	7843.45	10791.68	530.12	1899.03	2573.80	104.41	527.67
4.75	5030.41	5530.37	7314.20	160.29	1014.77		-50.43	198.46
5.00	4172.42	3846.84	4927.44	-31.70	506.68	778.08	-110.75	38.23
5.25	3417.29	2638.94	3296.71	-120.68	222.01	396.50	-124.75	-33.64
5.50	2766.14	1783.55	2187.65	-152.53	68.10	181.16	-117.89	-60.73
5.75	2214.92	1185.27	1437.08	-154.53	-10.63	63.20	-103.09	-66.16
6.00	1755.80	771.94	931.92	-142.36	-47.12	1.49	-86.62	-61.95
6.25	1378.76	489.96	594.10	-124.68	-60.61	-28.29	-71.20	-54.16
6.50	1072.95	300.26	369.91	-106.05	-62.15	-40.41	-57.87	-45.69
6.75	827.60	174.55	222.51	-88.65	-57.97	-43.13	-46.78	-37.81
7.00	632.70	92.78	126.76	-73.37	-51.48	-41.14	-37.78	-30.99
7.25	479.26	40.81	65.52	-60.42	-44.44	-37.11		
7.50	359.47	8.79	27.17	-49.67	-37.75	-32.40	-24.80	-20.65
7.75		-10.05	3.88	-40.85				
8.00	195.46	-20.35	-9.63	-33.67	-26.60	-23.54	-16.56	-13.86
8.25		-25.22						
8.50	100.11	-26.74	-20.16					
9.00	46.52	-24.72	-20.54	-16.13	-13.08	-11.76	-7.87	-6.58
9.50	17.60	-20.34	-17.59					
10.0	2.82	-15.92	-14.05	-8.28	-6.73	-6.03	-4.06	-3.38
10.5	-4.09							
11.0	-6.79	-9.27			-3.68	-3.27	-2.23	
11.5	-7.36							
12.0	-6.92	-5.40	-4.83	-2.65	-2.13	-1.87	-1.31	-1.07
12.5	-6.10							
13.0	-5.18						-0.80	

14.0	-3.55
15.0	-2.38

TABLE II. Potential energies (in μE_h) for Σ states.

$r(a_0)$	$NaHe(^2\Sigma^+)$	$MgHe(^1\Sigma^+)$	$AlHe(^2\Sigma^+)$	$SiHe(^3\Sigma^-)$	$PHe(^4\Sigma^-)$	$SHe(^3\Sigma^-)$	$ClHe(^2\Sigma^+)$	$ArHe(^1\Sigma^+)$
2.50	95683.30	121183.91	196982.55	84553.80	209208.02	335317.72	153411.92	269746.28
2.75	56926.64	82777.45	158056.83	53471.73	149400.03	233077.89	97955.39	170955.83
3.00	35605.28	59875.81	128252.66	35265.00	105390.82	159039.66	62019.58	106606.79
3.25	23732.29	45110.71	102490.93	23677.79	73300.68	106974.92	38820.26	65563.98
3.50	16931.01	34758.27	80388.98	15852.27	50279.01	71152.27	23946.50	39801.87
3.75	12830.67	26990.11	62102.66	10429.88	34043.24	46891.42	14509.48	23843.90
4.00	10166.85	20919.42	47413.02	6674.28	22771.86	30652.77	8600.80	14076.16
4.25	8279.15	16097.97						
4.50	6831.28	12267.71	26948.07	2410.32	9834.96	12793.63	2752.31	4634.37
4.75	5656.17	9249.18						2551.32
5.00	4671.82	6897.51	14974.19	622.46	4033.16	5149.17	686.98	1342.16
5.25	3836.93	5088.00		211.57				654.08
5.50	3128.40	3712.42	8189.70	-20.43	1539.68	1964.11	37.32	272.89
5.75	2530.53	2678.96		-140.26			-74.50	69.73
6.00	2030.40	1910.87	4416.30	-192.33	516.44	679.13	-122.07	-32.00
6.25	1616.02	1346.10		-205.36		371.89	-134.99	-77.34
6.50	1276.01	935.01	2344.31	-197.34	122.03	184.81	-130.39	-92.40
6.75	999.61	638.83	1695.77	-179.21	34.55	73.63	-117.90	-92.06
7.00	776.87	427.66	1219.44	-157.34	-14.50	9.89	-102.77	-84.59
7.25	596.86	278.76	870.76		-39.92	-24.64	-87.67	-74.45
7.50	457.72	175.05	616.48	-114.75	-51.13	-41.50	-73.86	-63.94
7.75			431.85		-54.08	-47.95	-61.80	
8.00	259.93	55.74	298.47	-80.92	-52.47	-48.50	-51.53	-45.48
8.25						-45.90		
8.50	140.93	3.53	134.35	-56.59	-43.64	-41.82		
9.00	71.46	-16.36	52.16	-39.75	-33.62	-32.64	-25.10	-22.35
9.50	32.25	-21.56	12.86	-28.24				
10.0	11.02	-20.69	-4.51	-20.34	-18.60	-18.12	-12.86	-11.44
10.5	0.19	-17.73	-11.02					
11.0	-4.81	-14.43	-12.40	-11.06		-9.97	-7.01	-6.22
11.5	-6.67		-11.58					
12.0	-6.92	-8.99	-9.98	-6.37	-5.91	-5.67	-4.06	-3.59
12.5	-6.43							
13.0	-5.65		-6.70					
14.0	-4.02							
15.0	-2.75							

TABLE III. Potential energies (in μE_h) for Σ states.

$r(a_0)$	$KHe(^3\Sigma^+)$	$CaHe(^1\Sigma^+)$	$GaHe(^2\Sigma^+)$	$GeHe(^3\Sigma^-)$	$AsHe(^4\Sigma^-)$	$SeHe(^3\Sigma^-)$	$BrHe(^2\Sigma^+)$	$KrHe(^1\Sigma^+)$
2.25					367934.75	555557.44		
2.50	241499.56	213534.38	237968.52	117072.49	255312.73	398759.78	211380.27	357316.28
2.75	149055.59	132704.16		70646.03	178502.16	280959.12	136393.58	235435.55
3.00	91589.22	84754.82	142451.50	43870.95	124813.50	195425.72	87885.17	152807.17
3.25	56591.62	56657.86	106213.20	27649.20	86812.77	134315.61	56313.04	97814.81
3.50	35587.14	40126.67	81546.38	17426.12	59907.04	91370.48	35761.79	61822.05
3.75	23094.44	30120.60	61072.50	10835.26	40976.64	61614.90	22440.73	38598.16
4.00	15676.14	23692.23	45517.41	6561.30	27774.91	41231.97	13871.41	23798.46
4.25				3810.83				
4.50	8488.72	15759.09	25027.83	2071.57	12408.81	18077.33	4982.80	8664.59
4.75				1000.84				5085.70
5.00	5503.37	10589.83	13639.52	366.03	5317.57	7691.36	1560.30	2908.22
5.25				9.24				1602.05
5.50	3883.86	6865.73	7380.82	−175.16	2155.69	3144.75	340.57	831.88
5.75				−256.29			90.89	387.80
6.00	2778.37	4257.53	3959.88	−278.29	797.93	1206.04	−40.45	139.44
6.25	2336.68	3299.19	2887.87	−268.61			−102.71	6.79
6.50	1953.21	2530.56	2098.13	−243.80	242.51	407.56	−125.96	−58.80
6.75	1621.58	1921.63	1517.31	−213.45	110.60	214.22	−128.17	−86.49
7.00	1336.75	1444.64	1091.06	−182.75	31.82	96.03	−119.91	−93.63
7.25	1094.15	1074.87	779.07	−154.28	−13.20	25.88	−107.17	−90.10
7.50	889.29	790.99	551.47	−129.13	−37.09	−13.92	−93.24	−82.00
7.75	717.76	575.06	386.09		−48.06	−34.86	−79.81	−72.10
8.00	575.31	412.32	266.49	−89.41	−51.35	−44.31	−67.66	−62.29
8.25					−50.29			
8.50	361.90	200.83	119.10	−61.85	−46.94	−45.82		
9.00	220.98	87.22	45.18	−43.18	−37.85	−38.62	−33.98	−31.95
9.50	130.35	29.00	9.84	−30.56				
10.0	73.50	1.08	−5.68	−21.98	−21.79	−22.82	−17.49	−16.44
10.5		−10.84	−11.36					
11.0	18.08	−14.71	−12.40	−11.94	−12.20	−12.78		−8.90
11.5	6.30	−14.80	−11.46					
12.0	−0.11	−13.31	−9.83	−6.89	−7.02	−7.30	−5.47	−5.09
12.5	−3.34	−11.34						
13.0	−4.67	−9.39	−6.57		−4.21	−4.33		
13.5	−5.00							
14.0	−4.79	−6.21						
14.5	−4.35							
15.0	−3.81	−4.06			−1.70			

TABLE IV. Potential energies (in μE_h) for Σ states at large r.

$r(a_0)$	LiHe($^2\Sigma^+$)	NaHe($^2\Sigma^+$)	KHe($^2\Sigma^+$)
16.0	−1.60	−1.87	−2.79
17.0			−1.99
18.0	−0.76	−0.89	−1.41
20.0	−0.39	−0.46	−0.73
22.0	−0.22	−0.25	
24.0		−0.15	

TABLE V. Potential energies (in μE_h) for Π states.

$r(a_0)$	$BHe(^2\Pi)$	$CHe(^3\Pi)$	$OHe(^3\Pi)$	$FHe(^2\Pi)$	$AlHe(^2\Pi)$	$SiHe(^3\Pi)$	$SHe(^3\Pi)$	$ClHe(^2\Pi)$
2.50	62042.01	152551.33	80713.69	125012.48	108560.46	214791.39	184325.77	303926.03
2.75	45457.29	102492.14	48243.81	72839.15	72090.98	163643.44	124297.33	201130.75
3.00	32641.40	67872.08	28331.92	42104.34	50240.50	122883.98	82862.04	130832.90
3.25	22832.58	44411.96	16323.75	24126.85	35991.27	90824.70	54518.89	83944.00
3.50	15552.33	28754.54	9202.93	13679.92	26011.82	66158.80	35374.72	53233.49
3.75	10325.13	18432.53	5051.74	7652.25	18718.05	47593.30	22622.26	33396.28
4.00	6683.55	11696.42	2675.40	4203.52	13306.48	33879.04	14246.13	20726.49
4.50	2578.12	4556.42	614.39	1159.12	6380.92	16727.10	5353.24	7694.89
4.75	1520.11	2784.73		559.71				
5.00	851.42	1669.74	35.75	238.43	2803.19	8013.80	1815.01	2667.20
5.25	439.46	975.35	-53.68	72.30		5485.08		
5.50	193.24	548.25	-88.27	-8.76	1089.07	3723.41	496.34	811.32
5.75	51.80	289.62	-95.36	-44.24		2503.64		403.22
6.00	-24.85	136.19	-89.71	-56.14	333.48	1664.38	49.73	169.43
6.25	-62.50	47.72	-79.06	-56.45		1090.75	-34.74	40.29
6.50	-77.36	-1.14	-67.27	-51.62	33.81	701.62	-74.81	-27.03
6.75	-79.57	-26.26	-56.13	-44.97	-31.11	439.91	-89.64	-58.61
7.00	-75.19	-37.47	-46.33	-38.15	-65.29	265.72	-90.78	-70.13
7.25	-67.83	-40.79	-38.06		-80.38		-85.02	-70.89
7.50	-59.51	-39.86	-31.21	-26.44	-84.06	77.27	-76.28	-66.30
7.75	-51.32	-36.82			-81.28		-66.72	-59.42
8.00	-43.79	-32.91	-21.09	-18.06	-75.15	1.84	-57.45	-51.94
8.25							-49.01	
8.50	-31.40				-59.65	-23.90	-41.58	
9.00	-22.40	-18.32	-10.06	-8.64	-45.05	-29.05	-29.77	-27.44
9.50	-16.07				-33.35	-26.59		
10.0	-11.65	-9.72	-5.18	-4.42	-24.58	-21.97	-15.48	-14.25
10.5					-18.18			
11.0			-2.85	-2.41	-13.57	-13.43	-8.45	-7.74
11.5					-10.24			
12.0	-3.69	-3.05	-1.66	-1.39	-7.81	-7.93	-4.86	-4.43
12.5								
13.0				-0.84	-4.71			

TABLE VI. Potential energies (in μE_h) for Π states.

$r(a_0)$	GaHe($^3\Pi$)	GeHe($^3\Pi$)	SeHe($^3\Pi$)	BrHe($^3\Pi$)
2.25			353799.12	
2.50	135413.39	257268.45	235893.92	380697.91
2.75		188215.56	158450.52	259028.05
3.00	57711.49	136903.31	106316.02	173784.59
3.25	38936.48	98994.61	70908.88	115101.68
3.50	26393.18	71092.17	46882.68	75371.41
3.75	17804.68	50706.20	30678.58	48848.66
4.00	11871.99	35939.66	19844.36	31349.58
4.25		25324.51		
4.50	4992.82	17741.05	7971.49	12522.06
4.75		12357.23		
5.00	1871.22	8557.98	2976.07	4755.60
5.25		5890.99		
5.50	554.63	4027.70	977.52	1667.37
5.75		2731.88		937.50
6.00	55.43	1834.98	230.47	495.31
6.25	−47.99	1217.33		232.88
6.50	−100.31	794.44	−18.79	81.57
6.75	−121.80	506.97	−63.38	−1.97
7.00	−125.46	313.36	−82.30	−44.88
7.25	−119.46	184.49	−86.69	−63.99
7.50	−108.78	99.96	−83.33	−69.61
7.75	−96.37		−76.25	−67.97
8.00	−83.90	11.50	−67.75	−62.74
8.50	−61.75	−20.70	−51.01	
9.00	−44.67	−28.83	−37.31	−36.50
9.50	−32.24	−27.57		
10.0	−23.41	−23.31	−19.74	−19.42
10.5	−17.18			
11.0	−12.76	−14.58	−10.79	
11.5	−9.61			
12.0	−7.33	−8.69	−6.20	−6.02
13.0	−4.43		−3.74	

TABLE VII. Potential energies (in μE_h) for Σ states.

$r(a_0)$	ZnHe($^1\Sigma^+$)	CdHe($^1\Sigma^+$)
2.50	143078.67	239242.92
3.00	68671.62	100731.95
3.50	35816.88	48440.83
4.00	18682.95	24846.64
4.50	9443.28	12864.53
5.00	4575.09	6530.08
5.50	2106.15	3199.84
6.00	905.34	1492.87
6.50	347.72	647.79
7.00	103.27	247.04
7.50	4.94	67.64
7.75	−16.85	22.27
8.00	−28.56	−5.68
8.25	−33.86	−21.97
8.50	−35.24	−30.60
9.00	−32.09	−34.94
9.50		−31.54
10.0	−20.53	−26.00
11.0	−11.95	−15.97
12.0	−6.96	−9.50
13.0	−4.17	−5.75
14.0	−2.59	−3.59

TABLE VIII. Parameters of potential-energy curves.

	state	r_0(Å)	r_e(Å)	$D_e(\mu E_h)$
Li–He	$^2\Sigma^+$	5.38	6.07	7.4
Be–He	$^1\Sigma^+$	4.02	4.53	26.8
B–He	$^2\Sigma^+$	4.13	4.64	21.1
	$^2\Pi$	3.12	3.54	79.8
C–He	$^3\Sigma^-$	2.62	2.99	156.2
	$^3\Pi$	3.44	3.86	40.9
N–He	$^4\Sigma^-$	3.02	3.40	62.5
O–He	$^3\Sigma^-$	3.18	3.57	43.1
	$^3\Pi$	2.69	3.03	95.4
F–He	$^2\Sigma^+$	2.46	2.78	124.8
	$^2\Pi$	2.89	3.24	57.3
Ne–He	$^1\Sigma^+$	2.70	3.03	66.5
Ne–He	$^2\Sigma^+$	5.56	6.27	7.0
Mg–He	$^1\Sigma^+$	4.53	5.09	21.7
Al–He	$^2\Sigma^+$	5.20	5.81	12.4
	$^2\Pi$	3.50	3.96	84.1
Si–He	$^3\Sigma^-$	2.90	3.31	205.4
	$^3\Pi$	4.24	4.76	29.1
P–He	$^4\Sigma^-$	3.66	4.11	54.1
S–He	$^3\Sigma^-$	3.73	4.18	48.8
	$^3\Pi$	3.24	3.65	91.5
Cl–He	$^2\Sigma^+$	2.94	3.32	135.1
	$^2\Pi$	3.38	3.78	71.5
Ar–He	$^1\Sigma^+$	3.31	3.49	94.1
K–He	$^2\Sigma^+$	6.34	7.14	5.0
Ca–He	$^1\Sigma^+$	5.31	5.96	15.1
Zn–He	$^1\Sigma^+$	3.99	4.49	35.2
Ga–He	$^2\Sigma^+$	5.17	5.78	12.42
	$^2\Pi$	3.24	3.68	125.7
Ge–He	$^3\Sigma^-$	2.78	3.19	278.4
	$^3\Pi$	4.30	4.83	29.0
As–He	$^4\Sigma^-$	3.79	4.26	51.4
Se–He	$^3\Sigma^-$	3.91	4.38	47.1
	$^3\Pi$	3.40	3.83	86.7
Br–He	$^2\Sigma^+$	3.12	3.52	129.0
	$^2\Pi$	3.57	3.99	69.7
Kr–He	$^1\Sigma^+$	3.32	3.71	93.6
Cd–He	$^1\Sigma^+$	4.20	4.73	35.0

TABLE IX. Parameters of RG–He interactions.

source	r_0(Å)	r_e(Å)	D_e(meV)
	Ne–He		
VVD(1999)[a]	2.699	3.032	1.823
CT(1999)[b]	2.701	3.028	1.811
present(a5z+bf)	2.700	3.029	1.809
Expt.[c]	2.70±0.01	3.03±0.02	1.80±0.05
	Ar–He		
CT(1999)[b]	3.131	3.492	2.562
present(a5z+bf)	3.129	3.494	2.560
Expt.[c]	3.11±0.01	3.48±0.02	2.55±0.07
	Kr–He		
present(5Z+bf)	3.317	3.711	2.548
present(a5z+bf)			2.567
Expt.[c]	3.30±0.01	3.69±0.02	2.54±0.07

[a]Reference 36.

[b]Obtained from the av5z results of Reference 37.

[c]Reference 38.

TABLE X. Van der Waals minima of certain atom–He interactions.

source	r_e(Å)	$D_e(\mu E_h)$
	Be–He	
CD(1982)[a]	4.77	25.5
HHS(1984)[b]	4.8	27.
LB(1999)[c]	4.65	26.
present	4.53	26.8
	Mg–He	
CD(1982)[a]	5.55	11.2
CSP(1987)[d]	5.66	10.4
FBSC(1989)[e]	5.16	21.
present	5.09	21.7
	Ca–He	
CRSP(1989)[f]	6.61	9.3
present	5.95	15.1
	Cd–He	
CSP(1987)[d]	5.2	42.3
present	4.73	35.0

[a]Obtained from the CEPA-2 results of Reference 39.

[b]Reference 40.

[c]Reference 41.

[d]Reference 42.

[e]Reference 43.

[f]Reference 44.

TABLE XI. Parameters of selected atom–He interactions.

source	state	r_0(Å)	r_e(Å)	$D_e(\mu E_h)$
		C–He		
LRR(1991)[a]	$^3\Sigma^-$	2.9	3.6	61.
	$^3\Pi$	3.8	4.7	14.
SF(1991)[b]	$^3\Sigma^-$	2.66	3.02	138.
	$^3\Pi$	3.49	3.87	36.
present	$^3\Sigma^-$	2.62	2.99	156.
	$^3\Pi$	3.44	3.86	41.
		O–He		
SJ(1985)[c]	$^3\Sigma^-$	3.24	3.61	37.
	$^3\Pi$	2.74	3.05	84.
present	$^3\Sigma^-$	3.18	3.57	43.
	$^3\Pi$	2.69	3.03	95.
		Cl–He		
NM(1998)[d]	$^2\Sigma^+$	2.98	3.37	121.
	$^2\Pi$	3.43	3.83	63.
BKBSCC(1998)[e]	$^2\Sigma^+$	2.96	3.34	132.
	$^2\Pi$	3.39	3.80	69.
present	$^2\Sigma^+$	2.94	3.32	135.
	$^2\Pi$	3.38	3.78	72.

[a]Reference 45.

[b]Reference 46.

[c]Reference 47.

[d]Obtained from the aqs results of Reference 48.

[e]Reference 49.

TABLE XII. Van der Waals minima of alkali–He interactions.

	$r_e(a_0)$	$D_e(\mu E_h)$
	Li–He	
DW(1971)[a]	11.6	7.4
Patil(1991)[b]	11.7	6.1
CLMTCD(1994)[c]	11.7	6.4
CRS(1995)[d]	12.2	8.
KTTY(1996)[e]	11.7	6.6
Staemmler(1997)[f]	11.49	7.24
present	11.47	7.36
	Na–He	
Patil(1991)[b]	12.1	5.5
CLMTCD(1994)[c]	12.1	5.9
KTTY(1996)[e]	12.2	5.9
present	11.85	6.96
	K–He	
Patil(1991)[b]	13.6	4.5
CLMTCD(1994)[c]	13.6	4.6
KTTY(1996)[e]	13.8	4.1
present	13.50	5.00

[a]Reference 50.

[b]Reference 51.

[c]Reference 52.

[d]Reference 53.

[e]Reference 54.

[f]Obtained from extrapolated results of Reference 55 as described in the text.

TABLE XIII. Diffusion integrals (in Å^2) for interactions of He with various atoms.

T(K)	Li	Be	N	Ne	Na	Mg	P	Ar	K	Ca	Zn	As	Kr	Cd
50	16.72	12.44	8.60	6.98	17.74	15.20	12.27	10.73	21.57	19.55	13.06	12.99	12.13	14.45
100	14.18	10.87	7.31	5.96	15.01	13.25	10.47	8.71	18.07	17.02	11.29	11.14	9.86	12.48
150	12.66	10.01	6.73	5.50	13.39	12.18	9.66	7.94	16.06	15.58	10.39	10.28	9.00	11.48
200	11.70	9.43	6.37	5.22	12.37	11.45	9.14	7.50	14.65	14.62	9.79	9.73	8.49	10.82
300	10.27	8.61	5.88	4.83	10.84	10.42	8.43	6.93	12.67	13.21	8.95	8.97	7.85	9.90
400	9.25	8.05	5.54	4.57	9.78	9.71	7.95	6.56	11.30	12.25	8.38	8.46	7.44	9.26
600	7.82	7.26	5.10	4.22	8.31	8.72	7.31	6.07	9.47	10.88	7.60	7.77	6.89	8.39
800	6.82	6.74	4.79	3.99	7.33	8.06	6.86	5.75	8.31	9.93	7.06	7.30	6.52	7.80
1000	6.05	6.30	4.55	3.80	6.60	7.51	6.51	5.48	7.47	9.18	6.64	6.92	6.22	7.33
1200	5.45	5.97	4.36	3.65	6.03	7.09	6.24	5.28	6.86	8.58	6.31	6.63	5.99	6.97
1500	4.76	5.56	4.13	3.47	5.40	6.58	5.89	5.03	6.19	7.86	5.91	6.26	5.71	6.53
2000	3.95	5.05	3.85	3.25	4.66	5.93	5.49	4.73	5.44	6.96	5.40	5.84	5.37	5.96
3000	3.02	4.33	3.45	2.94	3.79	5.04	4.91	4.29	4.59	5.76	4.70	5.22	4.88	5.23
4000	2.51	3.82	3.18	2.73	3.29	4.45	4.52	4.00	4.10	5.00	4.23	4.81	4.55	4.73
6000	1.96	3.13	2.81	2.44	2.73	3.67	3.97	3.60	3.54	4.08	3.60	4.23	4.09	4.06
8000	1.67	2.67	2.56	2.25	2.41	3.17	3.60	3.32	3.21	3.55	3.19	3.84	3.78	3.64
10000	1.49	2.32	2.36	2.11	2.19	2.83	3.32	3.11	2.97	3.19	2.89	3.55	3.54	3.33

TABLE XIV. Diffusion integrals (in Å^2) for interactions of He with various atoms.

T(K)	B	C	O	F	Al	Si	S	Cl	Ga	Ge	Se	Br
300	7.21	6.37	5.39	5.04	9.59	8.92	7.78	7.28	9.12	9.08	8.50	8.13
400	6.76	5.99	5.09	4.76	8.97	8.36	7.34	6.88	8.52	8.49	8.03	7.69
600	6.15	5.47	4.68	4.39	8.12	7.61	6.76	6.35	7.72	7.72	7.39	7.09
800	5.74	5.12	4.40	4.13	7.55	7.11	6.36	5.99	7.19	7.21	6.96	6.70
1000	5.41	4.84	4.18	3.93	7.10	6.71	6.05	5.71	6.77	6.81	6.62	6.38
1200	5.15	4.63	4.01	3.77	6.74	6.40	5.81	5.49	6.45	6.50	6.35	6.13
1500	4.82	4.35	3.81	3.58	6.31	6.03	5.51	5.22	6.06	6.11	6.02	5.83
2000	4.45	4.04	3.55	3.35	5.77	5.57	5.14	4.88	5.56	5.66	5.62	5.46
3000	3.90	3.59	3.19	3.02	5.03	4.93	4.62	4.42	4.90	5.03	5.06	4.95
4000	3.52	3.28	2.95	2.79	4.53	4.49	4.27	4.10	4.44	4.60	4.68	4.59
6000	3.00	2.85	2.61	2.49	3.85	3.89	3.79	3.66	3.83	4.02	4.15	4.10
8000	2.65	2.56	2.39	2.28	3.41	3.50	3.47	3.36	3.43	3.63	3.80	3.77
10000	2.39	2.35	2.22	2.12	3.08	3.20	3.21	3.14	3.14	3.34	3.53	3.52

TABLE XV. Viscosity integrals (in Å^2) for interactions of He with various atoms.

T(K)	Li	Be	N	Ne	Na	Mg	P	Ar	K	Ca	Zn	As	Kr	Cd
50	19.65	14.05	9.47	7.67	20.86	17.23	13.55	11.67	25.55	22.33	14.64	14.39	13.24	16.20
100	16.97	12.47	8.19	6.65	17.97	15.27	11.75	9.61	21.85	19.77	12.87	12.52	10.88	14.23
150	15.44	11.62	7.62	6.21	16.34	14.20	10.96	8.86	19.74	18.33	11.98	11.67	10.03	13.24
200	14.33	11.00	7.25	5.91	15.15	13.42	10.42	8.39	18.18	17.29	11.36	11.10	9.50	12.55
300	12.80	10.16	6.76	5.52	13.50	12.36	9.71	7.86	16.00	15.84	10.50	10.34	8.89	11.60
400	11.67	9.54	6.40	5.24	12.30	11.57	9.19	7.47	14.39	14.77	9.88	9.79	8.45	10.91
600	10.19	8.73	5.95	4.90	10.67	10.55	8.54	6.99	12.21	13.36	9.07	9.09	7.91	10.01
800	8.99	8.13	5.62	4.63	9.47	9.79	8.06	6.63	10.69	12.32	8.48	8.57	7.51	9.35
1000	8.04	7.69	5.37	4.44	8.57	9.22	7.69	6.37	9.60	11.51	8.03	8.19	7.22	8.86
1200	7.27	7.33	5.17	4.29	7.84	8.77	7.41	6.16	8.76	10.86	7.67	7.88	6.98	8.46
1500	6.38	6.89	4.92	4.10	7.03	8.20	7.05	5.90	7.88	10.04	7.23	7.50	6.69	7.98
2000	5.28	6.31	4.61	3.85	6.04	7.47	6.59	5.56	6.86	8.96	6.66	7.01	6.31	7.35
3000	3.98	5.52	4.17	3.52	4.86	6.45	5.96	5.10	5.72	7.47	5.88	6.34	5.80	6.49
4000	3.26	4.94	3.86	3.28	4.18	5.73	5.51	4.77	5.07	6.47	5.32	5.85	5.42	5.89
6000	2.52	4.16	3.46	2.97	3.44	4.77	4.92	4.34	4.37	5.26	4.59	5.24	4.94	5.12
8000	2.13	3.57	3.20	2.74	3.03	4.14	4.51	4.03	3.96	4.53	4.09	4.79	4.58	4.59
10000	1.89	3.14	2.95	2.58	2.75	3.69	4.18	3.80	3.67	4.06	3.72	4.45	4.32	4.21

TABLE XVI. Viscosity integrals (in Å^2) for interactions of He with various atoms.

T(K)	B	C	O	F	Al	Si	S	Cl	Ga	Ge	Se	Br
300	8.40	7.37	6.19	5.78	11.22	10.35	8.90	8.29	10.62	10.51	9.73	9.25
400	7.91	6.95	5.86	5.47	10.54	9.74	8.43	7.86	9.97	9.87	9.22	8.78
600	7.29	6.43	5.45	5.09	9.68	8.97	7.85	7.34	9.16	9.08	8.59	8.20
800	6.83	6.04	5.14	4.82	9.05	8.42	7.42	6.95	8.57	8.51	8.12	7.76
1000	6.49	5.76	4.92	4.61	8.57	8.01	7.10	6.66	8.13	8.10	7.77	7.44
1200	6.22	5.53	4.74	4.45	8.19	7.68	6.85	6.43	7.78	7.77	7.49	7.19
1500	5.88	5.25	4.52	4.24	7.72	7.28	6.53	6.15	7.35	7.37	7.15	6.88
2000	5.45	4.89	4.24	3.98	7.12	6.76	6.13	5.78	6.80	6.85	6.70	6.47
3000	4.84	4.39	3.85	3.62	6.28	6.05	5.57	5.28	6.05	6.15	6.09	5.91
4000	4.41	4.03	3.57	3.36	5.69	5.54	5.17	4.92	5.51	5.65	5.65	5.51
6000	3.84	3.56	3.20	3.03	4.91	4.88	4.65	4.45	4.82	5.00	5.09	4.98
8000	3.42	3.23	2.94	2.80	4.38	4.43	4.27	4.11	4.36	4.56	4.68	4.61
10000	3.11	2.98	2.75	2.62	3.98	4.08	4.00	3.86	3.99	4.21	4.38	4.33

TABLE XVII. Parameters[a] for He–atom interaction energies.

atom	ρ	α	C_6
Be	0.6821	2.058	12.84
N	0.4965	3.264	5.70
Ne	0.4162	3.960	2.98
Mg	0.7772	1.717	19.78
P	0.5997	3.168	14.69
Ar	0.4737	4.518	9.63
Ca	0.9038	1.459	35.34
Zn	0.6926	2.144	16.37
As	0.6190	3.170	17.16
Kr	0.5021	4.535	13.42
Cd	0.7214	2.223	22.31

[a]All values are in atomic units.

TABLE XVIII. Parameters[a] for like-atom interaction energies.

atom	ρ	a	C_6
Be	0.9430	1.771	206.83
N	0.5718	3.520	24.02
Ne	0.4112	5.001	6.08
Mg	1.1332	1.410	587.18
P	0.7781	3.359	161.36
Ar	0.5262	5.789	65.60
Ca	1.3863	1.204	2204.42
Zn	0.9639	1.907	338.20
As	0.8161	3.365	250.43
Kr	0.5830	5.707	130.89
Cd	1.0216	2.052	500.65

[a]All values are in atomic units.

TABLE XIX. Parameters of the atom–atom potential energy wells.

atom	σ(Å)	ϵ/κ(K)
	S states[a]	
Be	4.389	52.58
N	3.246	49.43
Ne	2.767	36.21
Mg	4.870	69.41
P	4.212	66.73
Ar	3.426	112.66
Ca	5.330	126.77
Zn	4.142	111.37
As	4.272	92.16
Kr	3.693	140.93
Cd	4.572	95.17
	P states[a]	
B	4.012	38.84
C	3.769	24.95
O	3.232	22.75
F	3.123	15.51
Al	4.590	81.01
Si	4.999	21.60
Cl	3.859	47.63
Ge	4.262	113.23
Ga	4.449	68.49
Br	4.133	58.70

[a]The quantities *S* and *P* specify the angular momentum of the separated atom.

FIGURES

FIG. 1. Comparison of the potential energies for interactions of a He atom with alkali and rare-gas atoms in the repulsive region. The curves are obtained from a spline fit to the calculated values of $V(r)$ listed in Ref. 35 for He–He and Tables I – III for the remaining interactions.

FIG. 2. Comparison of theoretical and experimental potential energies for interactions of a Helium atom with rare-gas atoms. The points represent the calculated data: the data from Ref. 36 is indicated by full circles, that from Ref. 37 by crosses, and that from Tables I – III by open circles. The solid curves are obtained from the HFD-B potential fits of Ref. 38 to measured data.

FIG. 3. Comparison of calculated potential energies for the interaction of He with Cl. The data points were obtained from Ref. 49 and the solid lines were obtained from spline fits to the values of Tables II and V.

FIG. 4. Comparison of theoretical potential energies for interactions of He with Li in the van der Waals region. The full and open circles represent the data from the calculations of Refs. 55 and 56, respectively. The solid line is obtained by a spline fit to the values listed in Tables I and IV.

FIG. 5. Comparison of measured and calculated total Li–He scattering cross sections. The dashed lines indicate the spread of values obtained from the beam experiment of Ref. 60. The solid line represents the values calculated using the $V(r)$ of Tables I and IV as described in the text.

FIG. 6. Deviation of D_0^c from D_0^e for RG–He mixtures. The dash-dot line is obtained from the D_0^e calculated from the potential energies of Ref. 38. The full and open circles are obtained from the measured values tabulated in Ref. 38 and the predicted values of Ref. 85, respectively, for D_0^e. The short and long dashed line is obtained from the D_0^e calculated from the HFD-B potential of Ref. 84.

FIG. 7. Deviation of $\eta^c(x)$ from $\eta^e(x)$ for a RG–He mixture with $x = 0.5$. The dash-dot and the short and long-dashed lines are obtained from the η^e calculated from the potential energies of Refs. 38 and 84, respectively, and the V^{b-b} described in the text. The dashed line is obtained from the values of η^e listed in Ref. 86.

FIG. 8. $V_{SR}(r)$ for the interactions of He with the RG atoms and the atoms of the nitrogen series. The data points represent the values calculated from the $V(r)$ of Tables I – III as described in the text. The dashed and solid curves are obtained from the repulsive parameters listed in Table XVII using Eq. (9b).

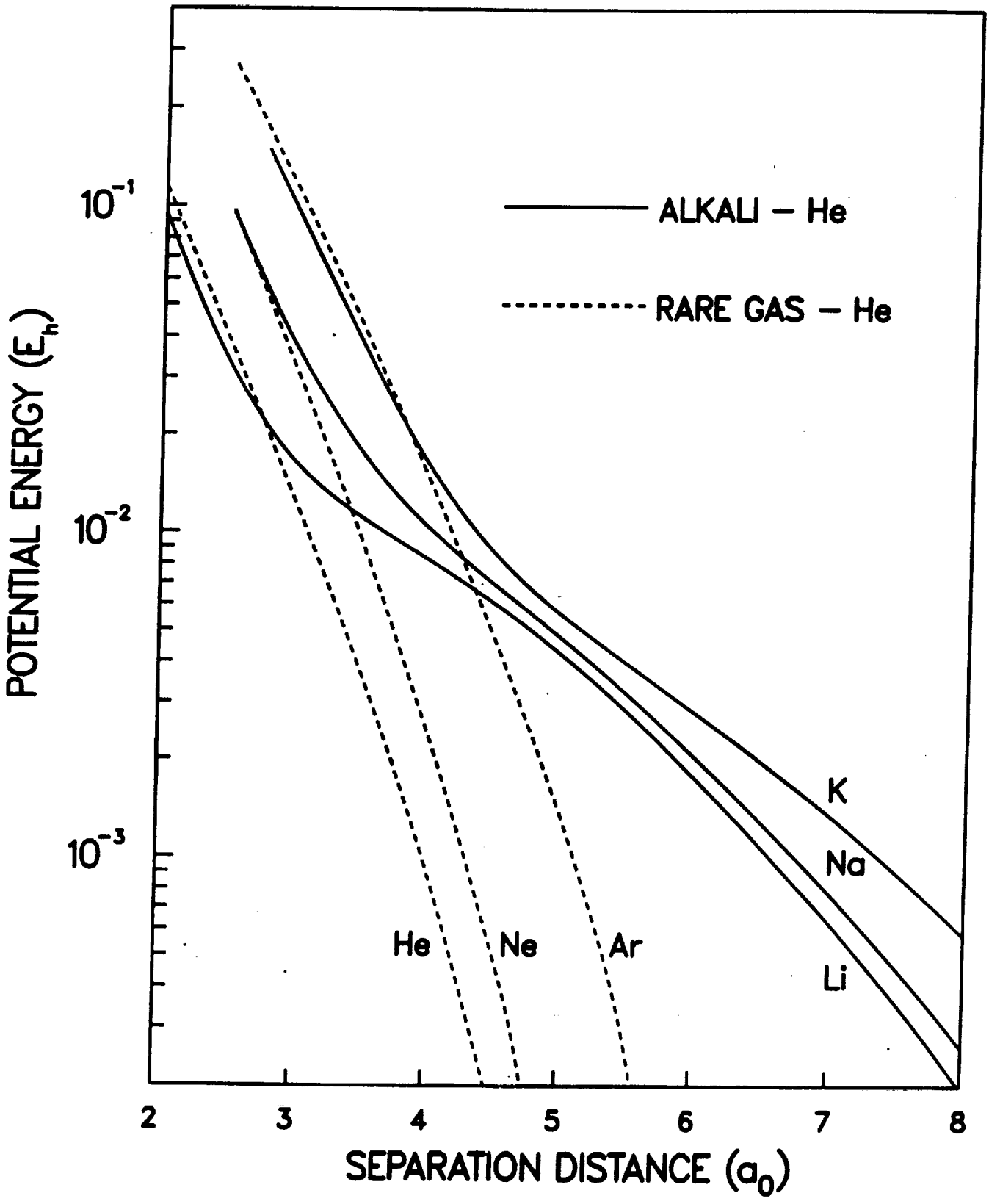
ALKALI – He
RARE GAS – He
POTENTIAL ENERGY (E_h)
10^{-1}
10^{-2}
10^{-3}
K
Na
Li
He
Ne
Ar
2
3
4
5
6
7
8
SEPARATION DISTANCE (a_0)

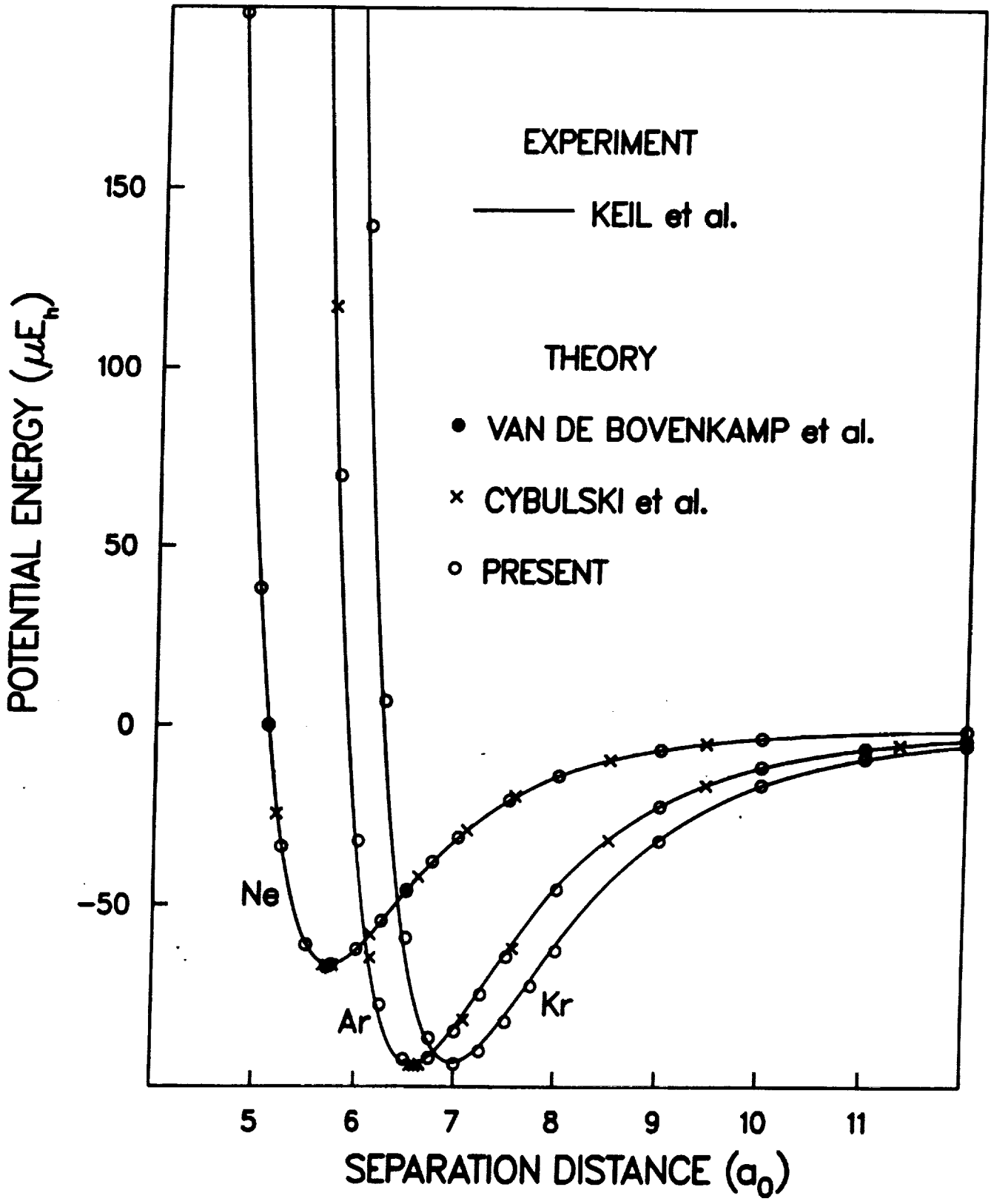
EXPERIMENT
KEIL et al.
THEORY
VAN DE BOVENKAMP et al.
CYBULSKI et al.
PRESENT
Ne
Ar
Kr
150
100
50
0
−50
5
6
7
8
9
10
11
POTENTIAL ENERGY (μE_h)
SEPARATION DISTANCE (a_0)

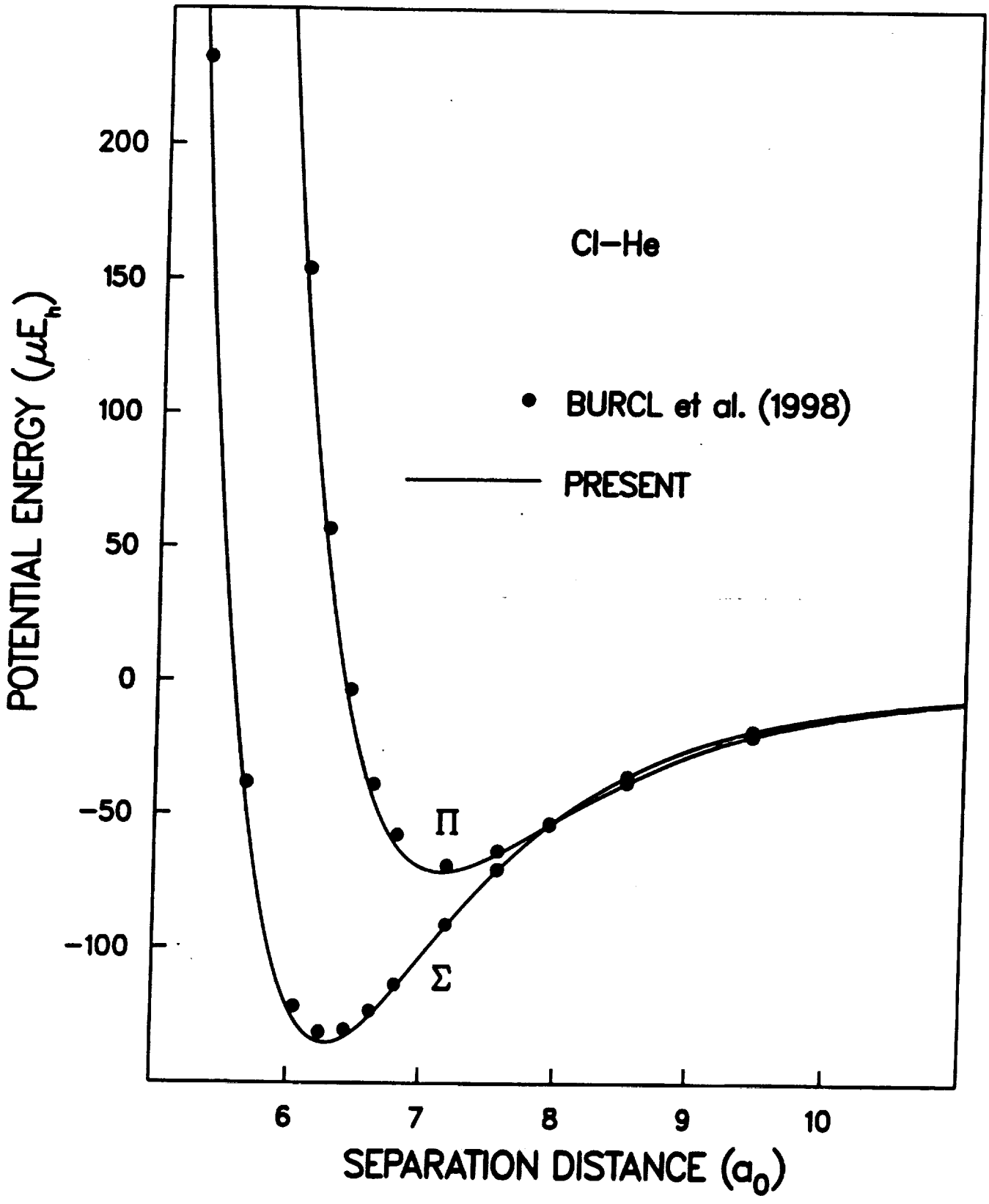
Cl–He
BURCL et al. (1998)
PRESENT
Π
Σ
POTENTIAL ENERGY (μE_h)
SEPARATION DISTANCE (a_0)
200
150
100
50
0
-50
-100
6
7
8
9
10

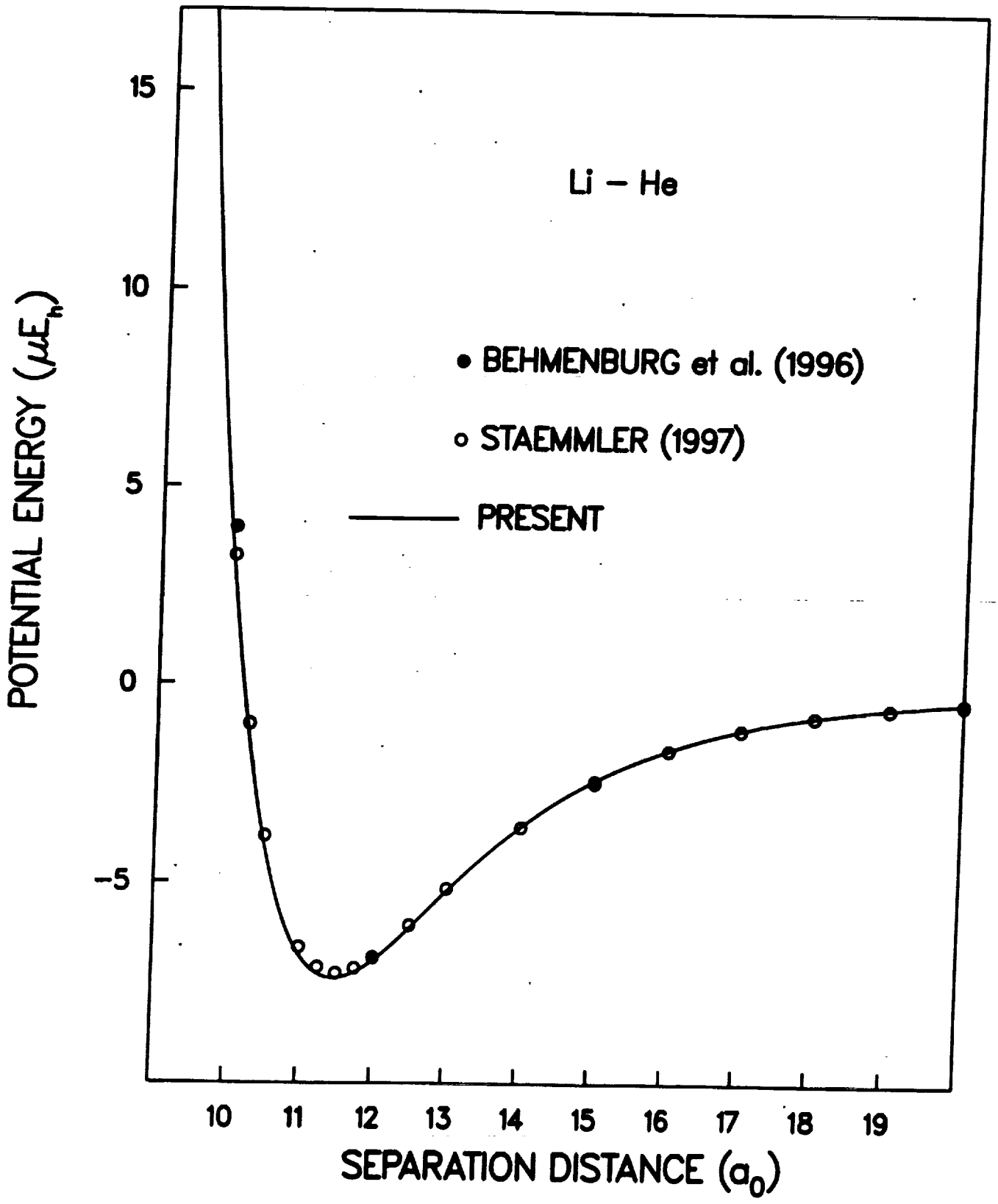
Li – He
• BEHMENBURG et al. (1996)
○ STAEMMLER (1997)
PRESENT
POTENTIAL ENERGY (μE_h)
SEPARATION DISTANCE (a_0)
15
10
5
0
−5
10
11
12
13
14
15
16
17
18
19

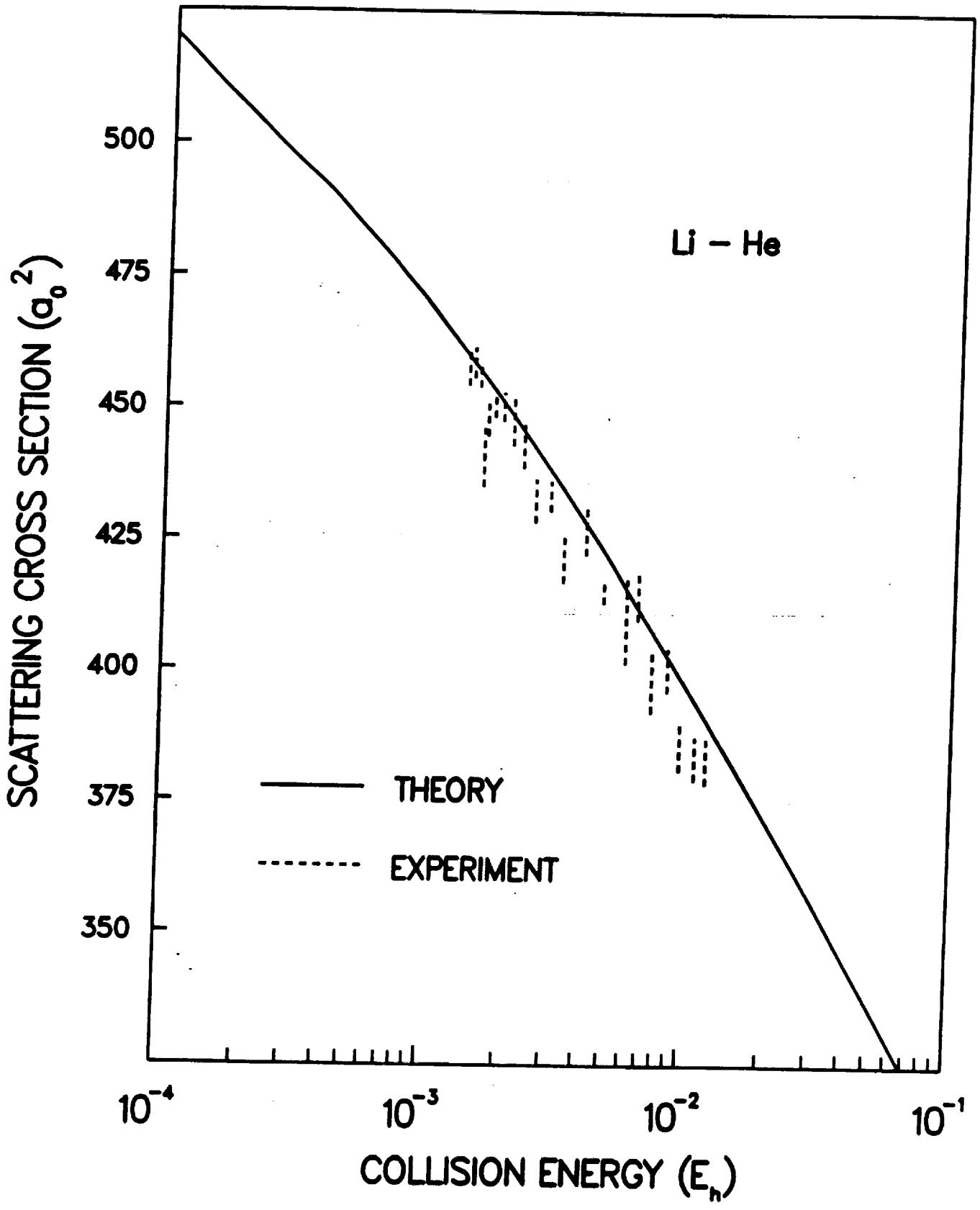
Li – He
SCATTERING CROSS SECTION (a_0^2)
500
475
450
425
400
375
350
THEORY
EXPERIMENT
10^{-4}
10^{-3}
10^{-2}
10^{-1}
COLLISION ENERGY (E_h)

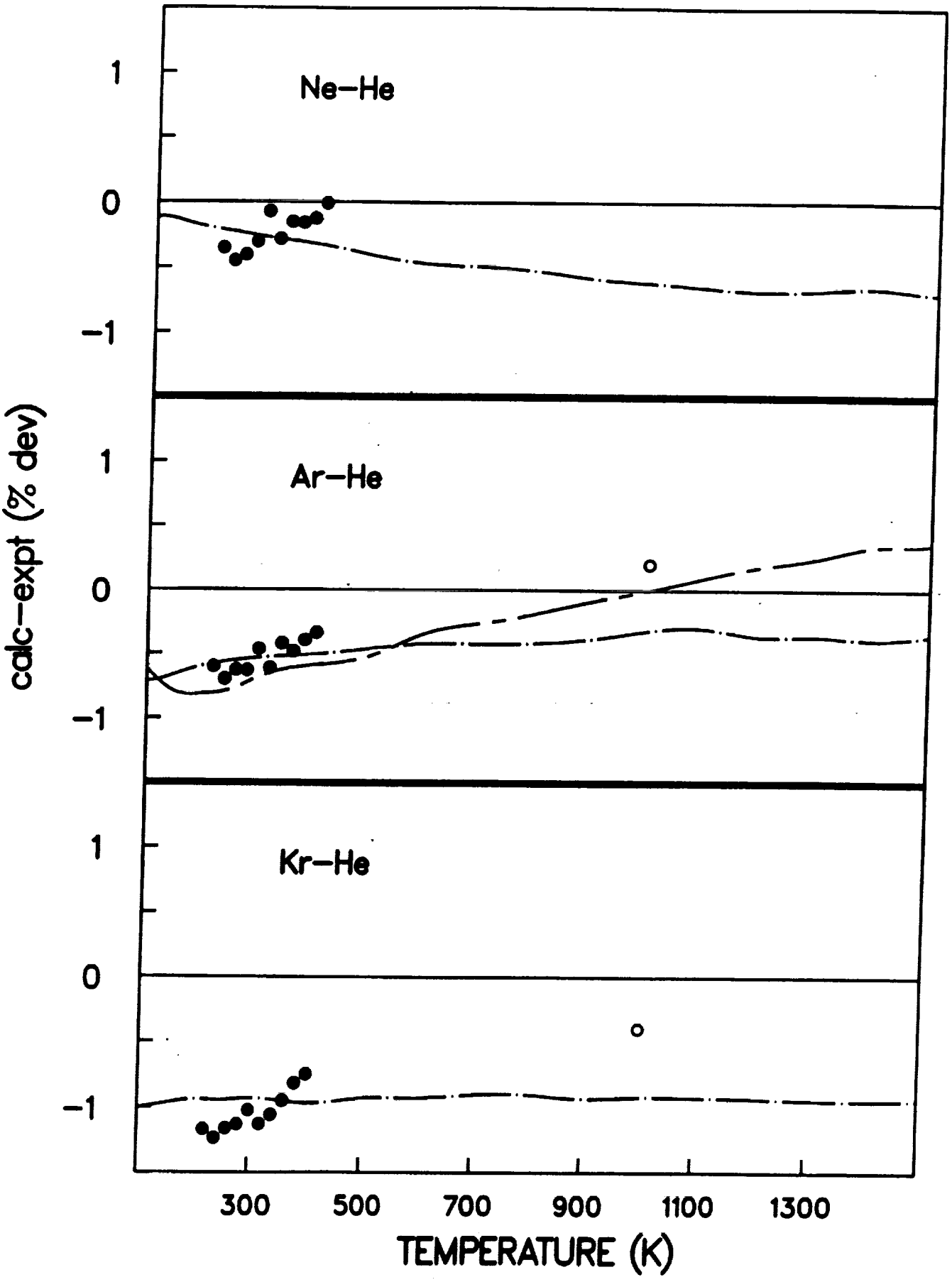
Ne–He
Ar–He
Kr–He
1
0
−1
calc–expt (% dev)
300
500
700
900
1100
1300
TEMPERATURE (K)

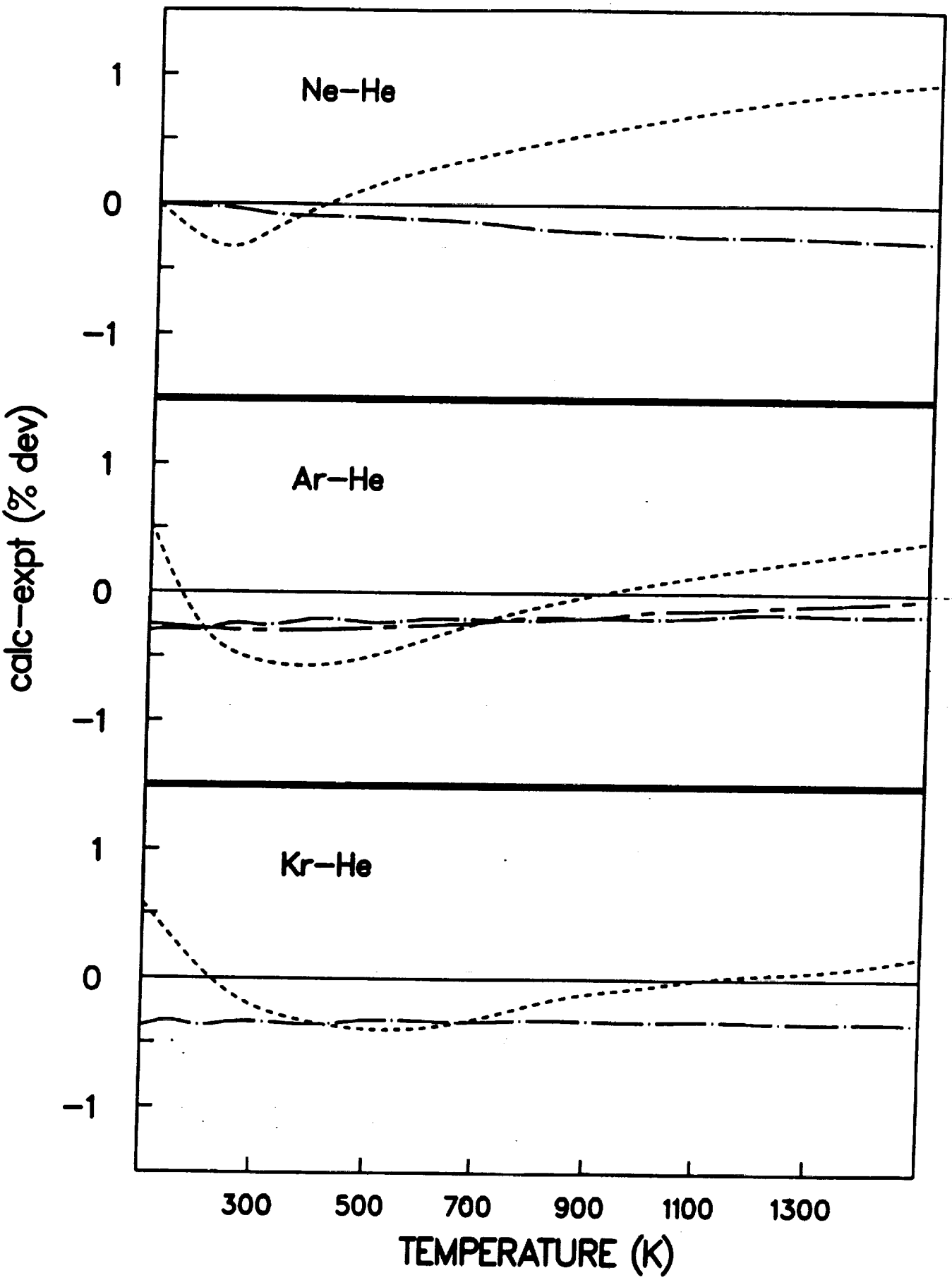
Ne–He
Ar–He
Kr–He
1
0
−1
calc–expt (% dev)
300
500
700
900
1100
1300
TEMPERATURE (K)

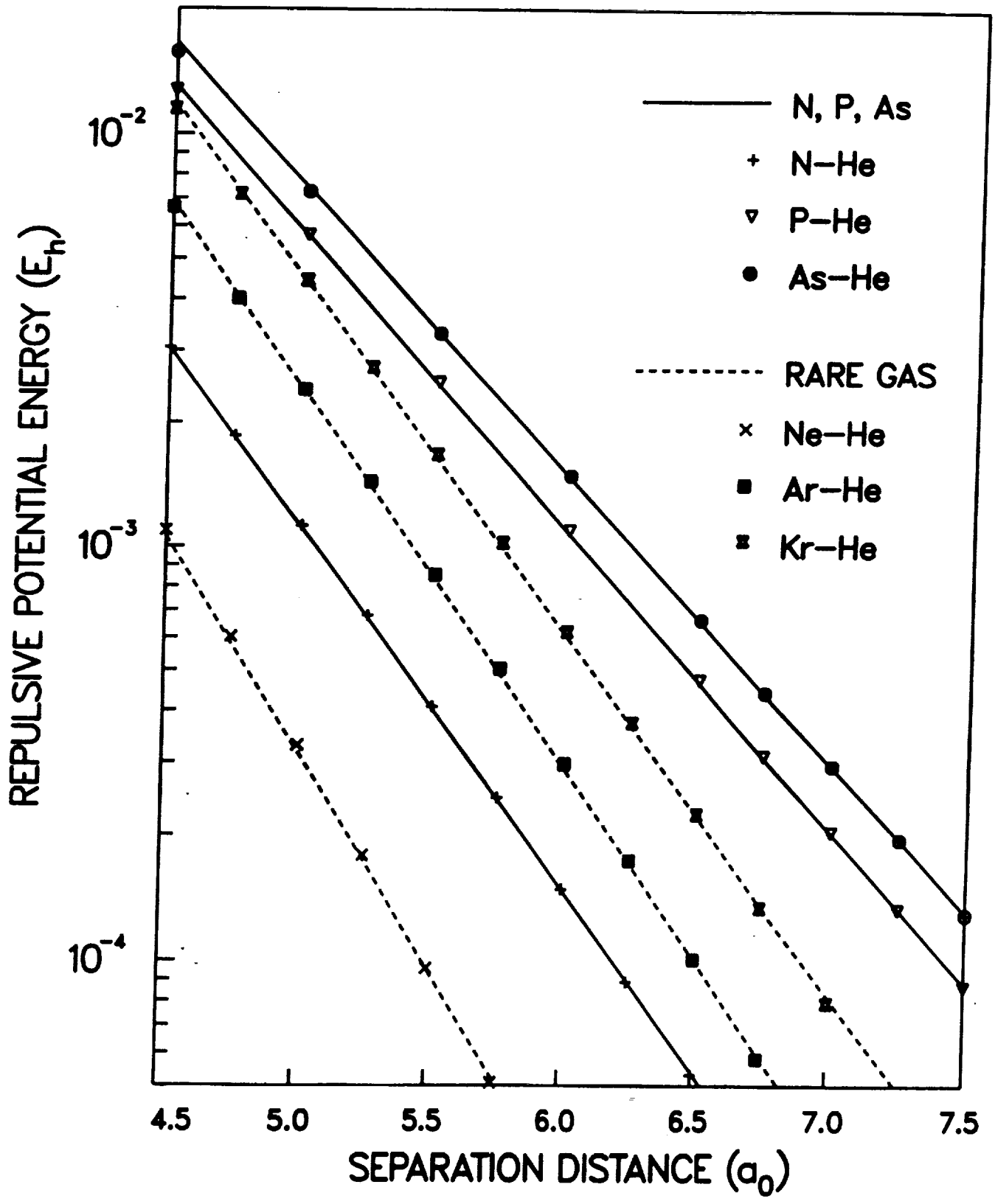
N, P, As
N–He
P–He
As–He
RARE GAS
Ne–He
Ar–He
Kr–He
REPULSIVE POTENTIAL ENERGY (E_h)
10^{-2}
10^{-3}
10^{-4}
4.5
5.0
5.5
6.0
6.5
7.0
7.5
SEPARATION DISTANCE (a_0)